Geomorphology 248 (2015) 33–46

Contents lists available at ScienceDirect

Geomorphology

journal homepage: www.elsevier.com/locate/geomorph

Soil genesis and evolution on calanchi (badland-like landform) of central Italy

Stefania Cocco [a,*], Giorgia Brecciaroli [a], Alberto Agnelli [b], David Weindorf [c], Giuseppe Corti [a]

[a] Dipartimento di Scienze Agrarie, Alimentari e Ambientali, Università Politecnica delle Marche, Via Brecce Bianche, 60131 Ancona, Italy
[b] Dipartimento di Scienze Agrarie, Alimentari e Ambientali, Università degli Studi di Perugia, Borgo XX Giugno 72, 06121 Perugia, Italy
[c] Department of Plant and Soil Science, Texas Tech University, Lubbock, TX, USA

A R T I C L E I N F O

Article history:
Received 22 June 2014
Received in revised form 17 July 2015
Accepted 18 July 2015
Available online 26 July 2015

Keywords:
Soil morphology
Water retention
COLE
Salt leaching
NaCl
Clay dispersion

A B S T R A C T

Calanchi are badland-like erosional landforms, common in the Mediterranean region, which form from accelerated erosion processes. The calanchi slopes, naked or differently vegetated, can be considered as formed by different ecological tesserae originated by the mutual interaction of several factors such as erosion, geomorphology, microclimatic conditions, vegetation, ground cover, and pedogenesis. However, information about pedogenesis is rather scarce mainly because the soils developing on calanchi slopes are incessantly disturbed by erosion processes. To understand the role of soil evolution on landslide erosion, we considered three land facets each one made up of four tesserae (T1 to T4), which represented the different steps of soil and vegetal evolution of calanchi. The soil of each tessera was described, sampled by genetic horizons, and the samples were characterized for their physical, mineralogical and chemical properties. Field observations and laboratory data suggest that pedogenesis in the calanchi badlands may progress until a critical threshold. Indeed, advanced plant colonization and *solum* development improve soil structure, increase soil organic matter, and favor redistribution of nutrients along the profile. The improvement of structure at depth fosters water storage and clay dispersion through soil leaching and reduction of ionic strength of the soil solution, making soil less stable. Depending on the slope gradient, the soil weight acquired during rainfall events may trigger landsliding, mudflows, or collapses that rejuvenate the surface.

1. Introduction

Badlands are worldwide erosional landforms represented by several types of geoforms such as rills, gullies, ravines, canyons, hoodoos, and pinnacles (Plummer et al., 2012). The formation of different badland morphologies is due to the type of sedimentary bedrock, especially texture and cementation degree, as well as climate. Among the types of badlands, "calanchi" are landforms mainly originated from accelerated erosion such as creep, landsliding, mudflows, slope collapse, and piping that form a network of rills and gullies with high internal disorder (Alexander, 1980, 1982; Battaglia et al., 2002). Further, they generally form on Miocene to Pleistocene soft to semi-coherent marine sediments (Battaglia et al., 2002). Calanchi occupy much of the Italian territory and are diffused across southern Europe and northern Africa.

The main factors inducing the formation or controlling the persistence of calanchi, as for the other badland-like morphologies, are 1) fine-grained and poorly consolidated or diagenized bedrock, 2) topography, and 3) climatic conditions such as high intensity rainfall events (e.g., Battaglia et al., 2002; Gallart et al., 2002, 2013; Godfrey et al., 2008; Alonso-Sarria et al., 2011; Martínez-Murillo et al., 2012). The diffusion of calanchi in the Mediterranean basin, in addition to these three factors, can be attributed to an intense soil use (Dramis et al., 1982; Guasparri, 1993; Torri et al., 1999, 2013; Corti et al., 2013). In this area, vulnerability to erosion was triggered by anthropogenic removal of evergreen oak woodland during the Holocene, so exposing erodible soils to climate rigors, favoring rain-splash and runoff, and activating processes of mass wasting such as creep, sliding, and flowage (e.g., Bryan and Yair, 1982; Imeson and Verstraten, 1988; King, 1990; Howard, 2009; Torri et al., 2013). Another key factor controlling the formation of badlands as well as calanchi is represented by pedogenesis. The presence of a relatively stable soil instead of a thin accumulation of unconsolidated material or "regolith" (e.g., Fairbridge, 1968; Gallart et al., 2002), derived from the weathering of the underlying mudrock, may prevent or limit badland formation (Gallart et al., 2002). Also mineralogical composition plays an important role in badland development as diverse clay minerals may differently affect soil dispersivity (Summa et al., 2007; de Santis et al., 2010) or mass movements (Kasanin-Grubin, 2012). However, as far as we know, there is no evidence about the importance of mineralogy on the formation of calanchi or other badland-like geoforms. As evidence of this, studying badlands from Dinosaur Park and Chinguacousy (Canada) and calanchi from an area across Tuscany and Marche (Italy), Kasanin-Grubin (2012) found that the Dinosaur Park badlands had a mineral composition

* Corresponding author.
E-mail address: s.cocco@univpm.it (S. Cocco).

http://dx.doi.org/10.1016/j.geomorph.2015.07.031
0169-555X/

very similar to the Italian calanchi, while it differed from that of Chinguacousy badlands because of the diverse composition of the parent material. Further, the Italian calanchi have often been remodeled or obliterated for agriculture purposes by the use of explosives (Pavari, 1911) or bulldozers (Calzecchi-Onesti, 1954; Rendell, 1986; Guasparri, 1993). Because of this, calanchi landscapes result from pedo-climatic and anthropic forces (Torri et al., 2013).

As for the other types of badlands, calanchi are subject to a geomorphic evolution that produces a mosaic of soil surfaces (Guàrdia et al., 2000; Lázaro et al., 2000; Regüés et al., 2000; Cantón et al., 2003). On calanchi slopes, the soil surface may be naked or differently vegetated, so that the landscape can be considered as formed by different ecological tesserae (sensu Forman and Godron, 1986). Indeed, each tessera originated by the mutual interaction of several factors such as erosion, geomorphology, microclimatic conditions, vegetation, ground cover, and pedogenesis. Among these factors, information about pedogenesis on calanchi is rather scarce. Consequently, little is known about the role of soil evolution on calanchi dynamics. This paucity in knowledge can be partly ascribed to the fact that in these landscapes the erosion processes responsible for soil removal are often rapid, while soil re-formation on the scalped surfaces is very slow. Further, selection of the site where to accomplish pedologic study can be difficult as calanchi landscapes are often formed by many different tesserae, some of which, at sites, may lack or disappear as a result of erosion or pedogenesis. In some cases, tesserae appear to be linked among themselves so to form a system of soil and vegetal evolution that describes a so called *land facet*, namely a “combination of ecotypes forming a pattern of spatial relationships, being strongly related to properties of at least one attribute” (Bridgewater, 1993). We hypothesized that integrating pre-existing studies with new field observations and lab data may highlight the relationships among tesserae and improve the understanding of the role of pedogenesis on the processes of accelerated erosion that affect these landscapes. To test this hypothesis, this study was concentrated on soil genesis of calanchi *land facets* and assessing the role of soil evolution on landslide erosion.

2. Materials and methods

2.1. Background information

Most of central and southern Italy is made up of territories covered by calanchi (Fig. 1), which originated from Plio-Pleistocene marine sediments composed of alternating beds of clay, marl-clay, silt clay and silt (Alexander, 1982; Moretti and Rodolfi, 2000). In some cases the summit of the calanchi is occupied by forests, but more often it has been remodeled (leveled) and plowed to cultivate vines, olive trees, and cereals (Fig. 2). Deep plowing has been responsible for greatly increasing erosional processes that have left the calanchi slopes almost barren (Phillips, 1998). The steep slopes around the leveled summit show features of accelerated erosion with dissected bare terrain intersected by a network of gullies (Battaglia et al., 2002). Whether or not the summit is leveled and cultivated, it may host different soils in function of dip slope and exposition. The dip slope surfaces with an NNW to NNE aspect have rather developed soils (mostly Inceptisols) with a thick grass vegetation cover or cultivations, while the anti-dip slopes with an SSW to SSE aspect have poor soils (mostly Entisols) and are almost barren (e.g., Fascetti et al., 1990; Del Prete et al., 1997). If not artificially remodeled, the more or less vegetated slopes tend to form sharp pinnacles that are at the mercy of strong erosion (Fig. 3). Materials eroded from the slopes accumulate into, and at the side of, braided streams

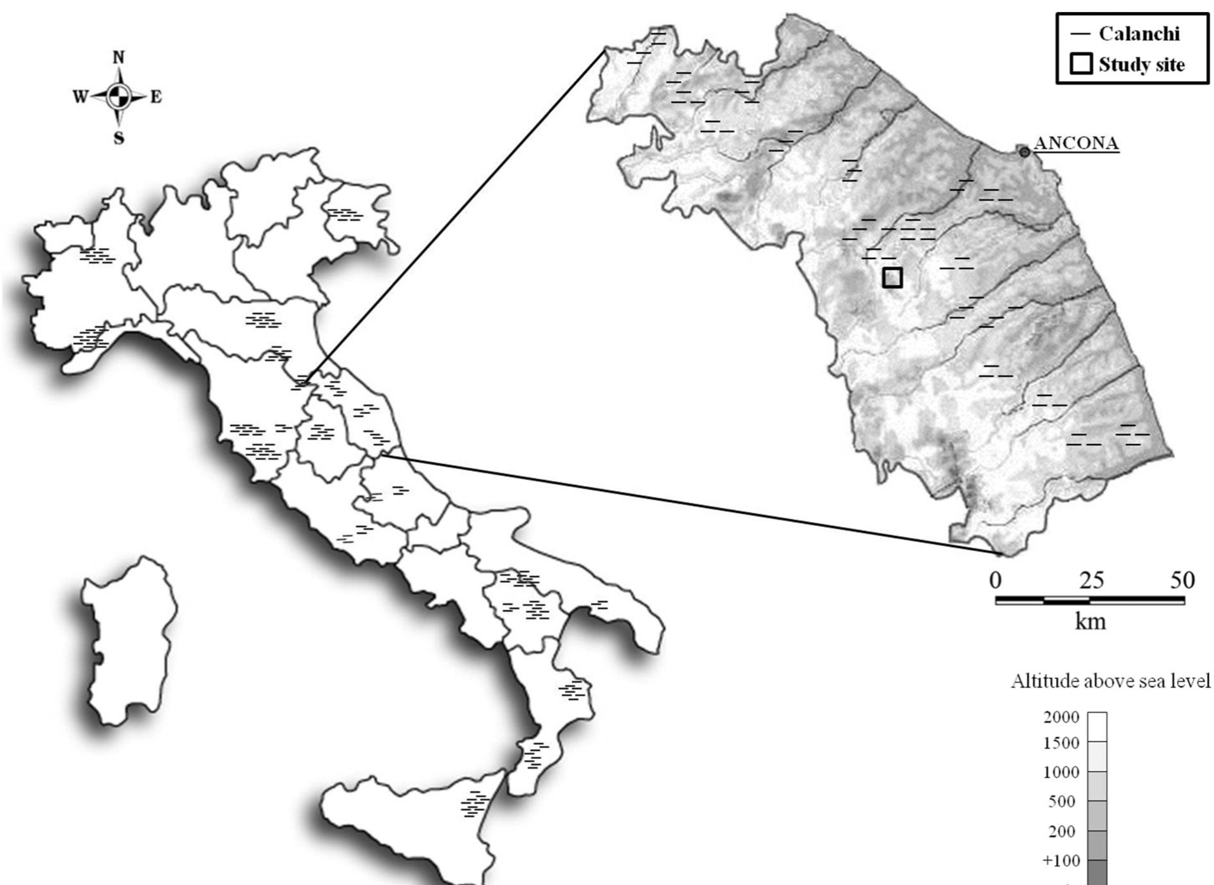

Fig. 1. Map of Italy with distribution of calanchi, magnification of the Marche region and indication of the study site.

Fig. 2. Example of remodeled (leveled) badlands for agricultural purposes at Rotorscio, Ancona, Italy.

where soils (Entisols and Inceptisols) develop also due to the colonization of shrubs and trees, sometimes with a thick understory.

In the Marche region (central Italy), calanchi landscapes are widespread, covering an area of ~100 km^2 all around the basin of the major rivers (Fig. 1). During surveys conducted in these valleys, we realized that, as in many other sites, the most common processes affecting calanchi were rilling, gullying, and slumping. Such occurrences were commonly preceded by a more or less rapid sequence of sheet erosion, micro-rilling, and landslides. The eroded material was deposited in footslopes, where shrubs (*Tamarix africana* Poiret, *Prunus spinosa* L., *Rosa canina* L., *Rubus ulmifolius* Schott, *Cornus sanguinea* L.) and a few trees (*Ulmus minor* Miller, *Salix alba* L.) developed. In many areas where pinnacles were remodeled during the 1920s and 1930s, we recognized four main tesserae along the flanks of the calanchi:

1) barren surface, which is usually in a slightly depressed position with respect to the other tesserae and was made up of a poorly developed soil (Entisol) with a "popcorn" surface;
2) semi-barren surface, which occupied micro-escarpments between the barren and vegetated tesserae, often in the shape of a crown

Fig. 3. Example of sharp pinnacles due to erosion, formed along the flanks of remodeled surface at Rotorscio, Ancona, Italy.

around the barren tessera, hosted sparse leguminous plants and a rather diffuse cover of a biological crust, and showed a slightly more developed soil than in the barren area (Entisol);

3) relatively well-vegetated surface, which usually occupied an area adjacent to the previous tessera, hosted a good grass cover of leguminous and gramineae plants and was made up of a rather developed soil (Inceptisol); and
4) well-vegetated surface, which hosted a thick vegetation cover made up of gramineae with few leguminous plants and shrubs, and a rather developed soil (Inceptisol). The soil of this tessera represented the highest stage of development on the steep slopes.

Hereinafter we refer to these four tesserae as T1, T2, T3 and T4, respectively.

2.2. Study site, field operations and sample preparation

We selected a study area of about 6 km^2 in the locality known as Coste di Staffolo, in the municipality of Staffolo (Ancona, Italy) (Fig. 1). Here, the lithology is represented by pelitic marine sediments made up of intercalated strata of shales, gray-blue marleous clay, and fine sand. The mean annual air temperature of the areas is ~13.5 °C, with July and August as the warmest months and January as the coldest one. The mean annual precipitation of the area is ~860 mm, concentrated during autumn and winter and with a summer drought. Several rainfall events with an intensity >50 mm h^{-1} occur annually, mainly in autumn and spring.

In the selected area, in orthogonal position with respect to the main slope, we observed many land facets as wide as meters or dozens of meters which, however, did not always show all the four tesserae. For our study, we chose three land facets with all the four tesserae that were 10–20 m wide, and had a similar SE to SSE exposure, an altitude between 198 and 220 m, and a general slope around 33–35°. The distance among the selected land facets ranged from 15 to 40 m. Table 1 reports the prominent features at one of the three land facets, and Fig. 4 shows a picture of the corresponding profiles. In each tessera of the three land facets, two soil profiles were opened. The profiles were described per Schoeneberger et al. (2002) and sampled by genetic horizons. The collected samples were air-dried and then sieved at 2 mm.

2.3. Soil analyses

Particle-size distribution was determined after the dissolution of organic cements by NaClO at pH 9 (Lavkulich and Wiens, 1970). Fine sand and very fine sand (250–100 and 100–53 μm, respectively) were recovered by wet sieving while silt was separated from clay by sedimentation maintaining the columns at 19–20 °C. Water retention at 33 kPa was determined by pressure plate extractor (Soil moisture Equipment Corp., Santa Barbara, CA). The coefficient of linear extensibility (*COLE*), which

Table 1
Morphological description of the land facet 2. Badlands of Coste di Staffolo, Ancona, Italy. For symbols see the legend at the bottom.

Landform: steep slope (about 35°) with diffuse soil cracks. Exposure: SSE. Altitude: 206 m. Mean annual air temperature: 13.5 °C. Mean annual precipitation: 860 mm. Parent material: Plio-Pleistocene fine-textured marine sediments. Soil classification according to Soil Survey Staff (2010).

	Depth	Color[a]	Texture[b]	Structure[c]	Roots[d]	Boundary[e]	Thickness	Other observations[f]
	cm						cm	
T1, soil with popcorn and barren surface: loamy, mixed, superactive, calcareous, mesic Udic Ustorthent.								
A1	0–2	2.5Y 7/2	sicl	3f,m abk	0	ci	2–4	Popcorn surface; w/d cracks
A2	2–5	2.5Y 4/2	sicl	3f,m abk	0	aw	2–3	2c
BC1	5–14	10YR 5/1	sicl	3th pl → f abk	0	cw	8–10	1c
BC2	14–23	2.5Y 5/2	sicl	3th pl → f abk	0	cw	8–9	–
BC3	23–32	2.5Y 5/1	sicl	3th pl → f abk	0	cw	9–11	–
C	32–40+	2.5Y 4/1	sicl	3m pl → f abk	0	–	–	–
T2, soil under sparse Hordeum maritimum, Hedisarium coronarium and biological crust: loamy, mixed, superactive, calcareous, mesic Udic Ustorthent.								
A1	0–2	2.5Y 7/2	sicl	3f,m abk	0	cw	2–3	crp cracks + w/d cracks
A2	2–4	10YR 4/2	sicl	3f,m abk	0	cw	2–3	crp cracks + w/d cracks; 2c
Bw	4–12	10YR 5/4	sicl	2f,m abk	2 mi,vf	aw	7–10	crp cracks + w/d cracks; 2c
BC1	12–20	10YR 5/3	sicl	2m,co abk	2 mi,vf,f	cw	6–8	1c
BC2	20–34	10YR 5/1	sicl	1m,co abk	2 mi,vf	cw	11–16	–
C	34–52+	2.5Y 2/2	sicl	2m pl → f abk	2 mi,vf,f	–	–	Roots mostly around the cracks
T3, soil with good cover made of Hedisarium coronarium and few gramineae: loamy, mixed, superactive, calcareous, mesic Udic Haplustept.								
A1	0–1	10YR 6/1	sicl	3f,m abk & 3f,m cr	0	ai	1–2	crp cracks
A2	1–4	2.5Y 5/2	sicl	3f,m,co sbk & 3f,m cr	0	cw	3–5	crp cracks partly filled by A material; 3c
Bw1	4–9	10YR 5/2	sicl	3f,m sbk-abk	1 mi,vf,f; v_1 m	cw	4–5	crp cracks partly filled by A material; 2c; 1sc
Bw2	9–7	10YR 5/2	sicl	3f,m sbk-abk	2 mi,vf,f; v_1 m	cw	5–8	crp cracks partly filled by A material; 2c; 1sc
Bw3	17–25	10YR 5/2	sicl	2–3m abk	3 mi,vf; 2 f	al	8–9	crp cracks partly filled by A material; 1c
BC	25–39	10YR 4/1	sicl	3m abk → th pl	2 mi,vf,f	al	11–14	crp cracks partly filled by A material
C	39–56+	2.5Y 4/0	sicl	2f,m pl → f abk	3 mi,vf,f	–	–	–
T4, soil with thick cover made of gramineae and leguminous: loamy, mixed, superactive, calcareous, mesic Typic Haplustept.								
Oi	5–0	–	–	–	–	cw	5–7	Remnants of grass
A1	0–4	5Y 4/2	sicl	3f,m,co cr	1 mi,vf,f	cw	4–5	crp cracks partly filled by O material; few M
A2	4–11	5Y 4/2	sicl	3f,m,co cr	2 mi,vf,f; 3 m	cw	7–9	crp cracks partly filled by O + A material; 3c; 1sc; few M
Bw1	11–18	2.5Y 4/2	sicl	3m,co abk	2 mi,vf,f,m	cw	6–7	crp cracks partly filled by A + O material; 3c; 1sc
Bw2	18–26	2.5Y 4/2	sicl	3m,co abk	2 mi,vf; 1 f,m	cw	6–8	crp cracks partly filled by A + O material; 2c; 1sc
Bw3	26–35	10YR 6/2	sicl	3m,co abk	3 mi,vf; 2 f,m	al	9–10	crp cracks partly filled by A + O material; 1c
BC1	35–47	2.5Y 5/2	sicl	3m,co abk	3 mi,vf,f	al	10–12	crp cracks partly filled by A + O material
BC2	47–59	2.5Y 4/2	sicl	3f,m,co abk → th pl	3 mi,vf; 2 f	cs	11–12	–
C	59–69+	2.5Y 2/2	sicl	2 f,m pl → f abk	2 mi,vf,f	–		–

[a] Moist and crushed, according to the Munsell Soil Color Charts.
[b] sicl = silty clay loam.
[c] 1 = weak, 2 = moderate, 3 = strong; th = thin, f = fine, m = medium, c = coarse; cr = crumb, abk = angular blocky, sbk = subangular blocky, pl = platy; → breaking into.
[d] 0 = absent, v_1 = very few, 1 = few, 2 = plentiful, 3 = abundant; mi = micro, vf = very fine, f = fine, m = medium, co = coarse.
[e] a = abrupt, c = clear; w = wavy, s = smooth, l = linear, i = irregular.
[f] w/d = wet/dry cycles, crp = creeping; 1 = thin, 2 = moderate, 3 = thick, c = cutans on the surface of the peds, sc = shiny cutans on the upper part of the roots; M = mesofauna.

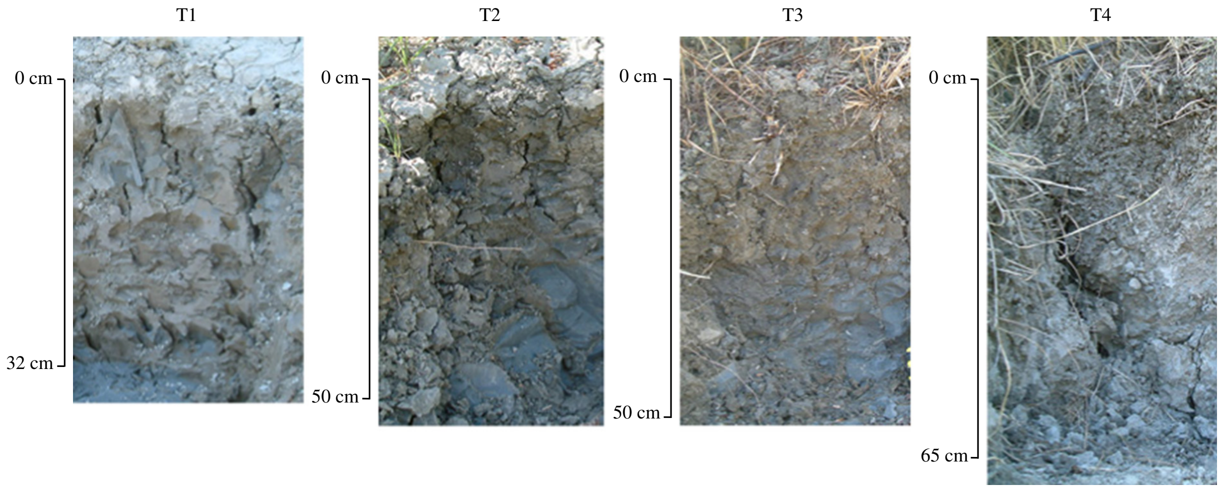

Fig. 4. Pictures of the T1 to T4 soil profiles forming one of the land facets under study at Coste di Staffolo, Staffolo municipality (Ancona, Italy). Images are not in scale among themselves.

is an estimate of soil swell–shrink potential, was determined according to the rod method of Schafer and Singer (1976), paying attention to obtain a similar fluidity for all pastes produced.

The content of carbonaceous minerals was chemically quantified by dissolution in 2 M HCl solution and successive titration of the evolved CO_2 (Bundy and Bremner, 1972). This method allows determining the content of carbonates with no interference due to the presence of gypsum. The attribution of the carbonates to calcite or dolomite was then made on the basis of their relative peak-areas obtained by X-ray diffractometric analyses. Crystalline minerals were identified by analyzing manually oriented powdered specimens on a Philips PW 1830 (Philips, Eindhoven, Holland) X-ray diffractometer, using Fe-filtered Co $K\alpha_1$ radiation (35 kV and 25 mA); the step size was 0.02° 2θ and the scanning speed was 1 s per step. Semi-quantitative estimation was obtained by identifying the minerals on the basis of their characteristic peaks. The content of the minerals was assessed from the area of the respective primary peaks, calculated by multiplying the peak height by the width at the half-height. Clay minerals were recognized after sub-samples were saturated with Mg and K, solvated with glycerol and heated at 330 °C and 550 °C. The peak-area of the mineral mixture made up of hydroxy-interlayered vermiculite and hydroxy-interlayered smectite (HIV/HIS), which fell in the range between 1.415 and 1.475 nm, was multiplied by a factor of 1.3 with respect to the 0.716–0.718 nm peak-area of kaolinite (Cuniglio et al., 2009).

The pH was determined potentiometrically in water (solid:liquid ratio 1:2.5). Total C and N contents were determined by a Carlo Erba EA1110 (Carlo Erba Instruments, Milan, Italy) dry combustion analyzer, while the organic C content was estimated by the Walkley–Black method without the application of heat (McLeod, 1975). The extractable (soluble plus exchangeable) Ca, Mg, K, Na and Cl were determined on aliquots of 2 g; each aliquot was placed into a centrifuge tube, submerged with 0.2 M NH_4NO_3 solution (solid:liquid ratio 1:10) and shaken for ~10 min (Corti et al., 1997). The suspension was left to rest for a while and then gently shaken to re-suspend the sediments and centrifuged. The extracted solution was filtered through Whatman 42 filter paper and analyzed by atomic absorption with a Shimadzu AA-6300 (Shimadzu, Tokyo, Japan)

Fig. 5. Surface of T2 soil sparsely colonized by *Hordeum marinum* Hudson and partly covered by a biological crust made of cyanobacteria, algae and lichens. Coste di Staffolo, Staffolo municipality (Ancona, Italy).

spectrophotometer for Ca, Mg, K and Na, and by the Mohr's silver nitrate titration method for Cl. The exchangeable sodium percentage (*ESP*) was calculated as Na / (Ca + Mg + K + Na) × 100.

2.4. Replicates and statistic

The results obtained for each horizon of the two profiles opened in each tessera were averaged. In the tables, the values reported for each horizon are the means of the three averages obtained for each tessera of the three land facets. The standard errors were calculated accordingly, using $n = 3$. Statistical analyses were performed by a two-way ANOVA and the means were compared to test the least significant difference at $P < 0.05$ by the Fisher's LSD test using XLSTAT PRO 7.5 software (XLSTAT, Addinsoft, New York, NY).

3. Results

3.1. Soil morphology

The T1 soil showed a bare "popcorn" surface (Kasanin-Grubin, 2012) forming a thin A1 horizon 2–4 cm thick interested by cracks due to wet/dry cycles (Table 1). Underneath the A1, there was an A2 horizon a few cm thick, three BC horizons with a thickness of ~10 cm each, and a C horizon. Even though all the horizons had a silty clay loam texture, the A1 and A2 horizons displayed a strongly developed angular blocky structure while the others showed a platy structure of sedimentary origin breaking into fine angular blocks. No roots were present in any of the T1 profiles, while clay cutans formed in the A2 and BC1 horizons. The soil of this tessera, which is dry below the depth of 25–30 cm only in mid-summer, was classified as a loamy, mixed, superactive, calcareous, mesic Udic Ustorthent (Soil Survey Staff, 2010).

The T2 was sparsely colonized by *Hordeum marinum* Hudson and *Hedisarium coronarium* L. and showed a surface partly covered by a black to blackish biological crust made up of cyanobacteria, algae and lichens (F. Rindi, personal communication, 2012) (Fig. 5). The soil was made up of two A horizons a few cm thick, a Bw horizon with a thickness of 8–10 cm, two BC horizons of 8–15 cm each and a C horizon of undefined thickness (Table 1). All the horizons had an angular blocky structure whose degree of development decreased with increasing depth. Roots were absent in the A horizons, but they were present in the underlying ones. Cracks due to creeping and wet/dry cycles interested A1, A2 and Bw horizons, and clay cutans formed only in the A2, Bw and BC1 horizons. The T2 soil, which is dry below the depth of 30–35 cm only in mid-summer, was classified as a loamy, mixed, superactive, calcareous, mesic Udic Ustorthent (Soil Survey Staff, 2010).

The T3 was well colonized by *H. coronarium* L. and few gramineae (surface cover was 90%), with a soil made of two A horizons a few cm thick, three Bw horizons that as a whole were 20 cm thick, and a BC horizon ~15 cm thick that rested on a C horizon (Table 1). The A1 horizon had a strongly developed structure made up of fine and medium angular blocks together with crumbs, while in the A2 horizon strongly developed sub-angular blocks with crumbs occurred. In the Bw1 and Bw2

Table 2
Particle-size distribution after NaClO treatment, water retention at 33 kPa and coefficient of linear extensibility (*COLE*) for the land facet forming the badlands of Coste di Staffolo, Ancona, Italy. Numbers in parentheses are the standard errors.

Horizons	Depth	Particle-size distribution in NaClO*				Water retention	*COLE*
		Sand		Silt	Clay	(at 33 kPa)	
		Fine	Very fine				
	cm	%				%	cm cm^{-1}
T1, soil with popcorn and barren surface							
A1	0–2	1(0)^{c}	4(1)^{ce}	73(4)^{ab}	22(3)^{h}	28.7(1.3)^{e}	0.248(0.002)^{ad}
A2	2–5	0(−)^{d}	3(1)^{df}	70(2)^{ad}	27(3)^{eh}	30.2(1.1)^{de}	0.258(0.026)^{a}
BC1	5–14	0(−)^{d}	3(0)^{df}	73(2)^{ab}	24(2)^{fh}	32.9(1.0)^{ad}	0.256(0.006)^{ab}
BC2	14–23	0(−)^{d}	1(0)^{f}	68(3)^{ae}	31(3)^{cf}	31.6(1.8)^{be}	0.258(0.021)^{a}
BC3	23–32	0(−)^{d}	2(0)^{ef}	69(2)^{ae}	29(2)^{ch}	32.8(1.4)^{ad}	0.258(0.008)^{a}
C	32–40+	0(−)^{d}	2(0)^{ef}	69(2)^{ae}	29(2)^{ch}	33.6(1.4)^{ad}	0.260(0.013)^{a}
T2, soil under sparse Hordeum maritimum, Hedisarium coronarium and biological crust							
A1	0–2	0(−)^{d}	3(1)^{df}	67(4)^{ae}	30(3)^{cg}	28.4(1.2)^{e}	0.194(0.008)^{eh}
A2	2–4	0(−)^{d}	4(1)^{ce}	62(2)^{cg}	34(3)^{ae}	28.5(1.4)^{e}	0.181(0.052)^{gh}
Bw	4–12	0(−)^{d}	3(1)^{df}	64(3)^{bf}	33(2)^{be}	29.1(1.4)^{de}	0.179(0.000)^{gh}
BC1	12–20	0(−)^{d}	3(1)^{df}	68(4)^{ae}	29(3)^{ch}	30.3(1.5)^{de}	0.203(0.013)^{dg}
BC2	20–34	0(−)^{d}	3(0)^{df}	74(2)^{a}	23(2)^{gh}	30.8(0.7)^{ce}	0.224(0.004)^{ag}
C	34–52+	0(−)^{d}	2(0)^{ef}	71(2)^{ac}	27(2)^{eh}	30.8(0.9)^{ce}	0.246(0.005)^{ad}
T3, soil under good cover made of Hedisarium coronarium and few Gramineae							
A1	0–1	1(0)^{c}	7(2)^{ab}	64(5)^{bf}	28(3)^{dh}	30.3(1.4)^{de}	0.115(0.001)^{i}
A2	1–4	1(0)^{c}	4(1)^{ce}	62(3)^{cg}	33(4)^{be}	31.0(1.4)^{ce}	0.126(0.020)^{i}
Bw1	4–9	1(0)^{c}	4(1)^{ce}	61(4)^{dg}	34(3)^{ae}	32.2(1.5)^{ae}	0.128(0.004)^{i}
Bw2	9–17	1(0)^{c}	5(1)^{bd}	63(4)^{cg}	31(3)^{cf}	33.7(1.5)^{ad}	0.148(0.007)^{hi}
Bw3	17–25	1(0)^{c}	5(0)^{bd}	66(2)^{af}	28(2)^{dh}	34.5(1.6)^{ac}	0.180(0.006)^{gh}
BC	25–39	0(−)^{d}	3(0)^{df}	66(2)^{af}	31(2)^{cf}	35.7(1.1)^{a}	0.187(0.010)^{fh}
C	39–56+	0(−)^{d}	3(0)^{df}	67(1)^{ae}	30(1)^{cg}	34.6(1.0)^{ac}	0.245(0.011)^{ad}
T4, soil under thick cover made of Gramineae spp.							
A1	0–4	5(1)^{a}	8(2)^{a}	59(5)^{eg}	28(2)^{dh}	35.3(2.4)^{ab}	0.210(0.008)^{bg}
A2	4–11	2(0)^{b}	4(1)^{ce}	54(5)^{g}	40(4)^{ab}	31.2(1.6)^{ce}	0.228(0.022)^{af}
Bw1	11–18	1(0)^{c}	6(2)^{ac}	57(4)^{fg}	36(2)^{ac}	29.9(0.8)^{de}	0.226(0.008)^{ag}
Bw2	18–26	1(0)^{c}	3(1)^{df}	62(3)^{cg}	34(2)^{ae}	30.6(1.1)^{ce}	0.232(0.015)^{af}
Bw3	26–35	1(0)^{c}	4(0)^{ce}	53(2)^{g}	42(2)^{a}	30.6(1.1)^{ce}	0.214(0.014)^{bg}
BC1	35–47	0(−)^{d}	3(0)^{df}	60(2)^{dg}	37(2)^{ac}	32.6(1.4)^{ae}	0.217(0.013)^{ag}
BC2	47–59	0(−)^{d}	3(0)^{df}	63(2)^{cg}	34(2)^{ae}	32.6(1.2)^{ae}	0.234(0.005)^{af}
C	59–69+	0(−)^{d}	2(0)^{ef}	71(2)^{ac}	27(2)^{eh}	n.d.	0.267(0.011)^{a}

In each column, mean values with different letters significantly differ for $P < 0.05$.
n.d. = not determined.
* Fine sand: 250–100 μm; very fine sand: 100–50 μm; silt: 50–2 μm; clay: <2 μm.

horizons, a well-developed sub-angular to angular blocky structure was present, while the Bw3 horizon showed only angular blocks. In the deepest horizons we observed primary structures that broke into secondary ones: in the BC horizon angular blocks broke into plates, while the contrary was true in the C horizon. Roots were absent in the A horizons and tended to increase with depth. Creeping cracks were abundant, reached the depth of ~40 cm and were partly filled by A material. Clay cutans formed in the A2 and Bw horizons, with a degree of development that tended to decrease with increasing depth. Thin shiny cutans covered the upper parts of the biggest roots in the Bw1 and Bw2 horizons. Because of the good vegetation cover, the T3 soil is usually dry below the depth of 30–35 cm from June to mid-September and was classified as a loamy, mixed, superactive, calcareous, mesic Udic Haplustept (Soil Survey Staff, 2010).

The T4 showed a 100% soil cover made by a thick vegetation of gramineae and leguminous species. The soil was composed of an organic horizon (Oi) ~5 cm thick, two A horizons with a whole thickness of 10–13 cm, three Bw horizons with a total thickness of ~25 cm, two BC horizons each one ~10 cm thick and a C horizon (Table 1). The A1 horizon showed a well-developed crumb structure, while the A2 horizon had a strongly developed structure made of fine and medium angular blocks and crumbs. The Bw horizons displayed a well-developed angular blocky structure, while in the BC horizons the angular blocks broke into plates and in the C horizon the contrary occurred. Roots were few in the A1 horizon but increased with depth. Creeping cracks were abundant, reaching the depth of ~50 cm, hosted few mesofauna and were partially filled by O and A materials. Clay cutans were present in the A2 and Bw horizons, with a thickness that tended to decrease with depth. Also in this case, thin shiny cutans covered the upper parts of the biggest roots in the A2, Bw1, and Bw2 horizons. Because of the thick vegetation cover, the T4 soil is usually dry below the depth of 45–50 cm from late spring to the end of summer and was classified as a loamy, mixed, superactive, calcareous, mesic Typic Haplustept (Soil Survey Staff, 2010).

3.2. Physical properties

Particle size-distribution (Table 2) substantially confirmed the field-determined textures with most of the horizons having a silty clay loam texture and the three upper horizons of T1 soil showing a silt loam texture. The amount of sand is usually < 10% in all the soils, while silt ranged from 53% to 74%. Clay content showed no difference with depth in T1, T2, and T3 soils, while T4 soil had the lowest value in the A1 horizon. As a whole, the clay content increased from T1 to T4 soils.

All water retention at 33 kPa data ranged from 28.4% to 35.7%, with slight significant differences among the soils (Table 2). The most marked difference occurred for the A1 horizon of the T4 soil, which showed the highest value among the A horizons. Throughout the profiles, the water retention was rather similar, except for a minimum tendency to increase with depth in T1 and T3.

COLE values tended to increase with depth in all soils (Table 2), as the highest values were expressed by the C horizons (from 0.245 to 0.260 cm cm^{-1}). However, a more defined increasing trend was observed in T2 and T3 than in T1 and T4 soils. By contrasting the whole soils, *COLE* was highest in T1 and lowest in T3.

Table 3
Semi-quantitative estimation of the mineralogical composition for the land facet forming the badlands of Coste di Staffolo, Ancona, Italy. Numbers in parentheses are the standard errors.

	C	D	G	Q	P	M	K	HIV/HIS	M–S	S	V	OM
	%											
T1, soil with popcorn and barren surface												
A1	23(1)^{ab}	3(1)^{a}	2(1)^{cd}	20(0)^{ac}	10(1)^{e}	8(0)^{d}	11(1)^{b}	14(2)^{a}	3(1)^{a}	3(0)^{a}	tr	3(0)
A2	23(1)^{ab}	3(0)^{a}	1(0)^{ce}	21(0)^{ac}	11(1)^{ce}	8(0)^{d}	12(1)^{ab}	13(2)^{a}	3(0)^{a}	2(1)^{a}	tr	3(0)
BC1	24(1)^{ab}	2(0)^{b}	tr	22(1)^{a}	11(1)^{ce}	9(0)^{c}	14(1)^{a}	12(1)^{a}	1(0)^{bc}	2(0)^{a}	1(0)^{b}	2(1)
BC2	23(1)^{ab}	2(0)^{b}	2(1)^{cd}	20(1)^{ac}	10(0)^{de}	10(0)^{b}	14(1)^{a}	13(2)^{a}	2(0)^{bc}	2(0)^{a}	1(0)^{b}	1(0)
BC3	23(0)^{ab}	2(0)^{b}	4(1)^{a}	20(1)^{ac}	10(0)^{de}	10(0)^{b}	14(1)^{a}	12(2)^{a}	tr	2(1)^{a}	tr	3(0)
C	23(0)^{ab}	2(0)^{b}	tr	21(1)^{ab}	13(0)^{ac}	10(0)^{b}	14(0)^{a}	12(2)^{a}	tr	2(1)^{a}	tr	2(0)
T2, soil under sparse Hordeum maritimum, Hedisarium coronarium and biological crust												
A1	24(1)^{ab}	2(0)^{b}	tr	20(1)^{ac}	11(1)^{ce}	9(0)^{c}	12(1)^{ab}	14(2)^{a}	2(0)^{ab}	2(0)^{a}	1(0)^{b}	2(0)
A2	24(1)^{ab}	3(0)^{a}	tr	20(1)^{ac}	11(0)^{ce}	8(0)^{d}	12(1)^{ab}	15(2)^{a}	1(1)^{bc}	2(0)^{a}	1(0)^{b}	2(1)
Bw	24(1)^{ab}	2(1)^{b}	tr	18(0)^{c}	15(1)^{a}	9(0)^{c}	13(1)^{ab}	13(2)^{a}	1(0)^{bc}	2(0)^{a}	1(0)^{b}	2(0)
BC1	23(1)^{ab}	2(0)^{b}	tr	19(2)^{bc}	14(1)^{ab}	10(0)^{b}	13(0)^{ab}	13(2)^{a}	1(0)^{bc}	3(0)^{a}	tr	1(0)
BC2	23(1)^{ab}	2(0)^{b}	4(1)^{a}	20(1)^{ac}	11(0)^{ce}	10(0)^{b}	13(0)^{ab}	13(2)^{a}	1(0)^{bc}	2(1)^{a}	tr	1(0)
C	23(1)^{ab}	2(0)^{b}	1(0)^{ce}	21(1)^{ab}	11(0)^{ce}	11(0)^{a}	14(0)^{a}	12(2)^{a}	1(0)^{bc}	2(0)^{a}	tr	2(0)
T3, soil with good cover made of Hedisarium coronarium and few Gramineae												
A1	23(1)^{ab}	tr	–	22(1)^{a}	11(1)^{ce}	9(0)^{c}	14(2)^{a}	13(2)^{a}	2(0)^{ab}	2(0)^{a}	2(1)^{a}	2(0)
A2	23(0)^{ab}	tr	3(1)^{ab}	22(0)^{a}	11(1)^{ce}	9(1)^{c}	14(1)^{a}	13(2)^{a}	1(0)^{bc}	2(0)^{a}	1(0)^{b}	1(0)
Bw1	23(1)^{ab}	1(0)^{c}	tr	21(0)^{ab}	12(1)^{ce}	10(0)^{b}	13(1)^{ab}	13(2)^{a}	1(0)^{bc}	2(0)^{a}	1(0)^{b}	3(1)
Bw2	23(1)^{ab}	1(0)^{c}	tr	21(1)^{ab}	13(1)^{ac}	10(0)^{b}	14(1)^{a}	12(2)^{a}	1(0)^{bc}	2(0)^{a}	1(0)^{b}	2(0)
Bw3	22(1)^{b}	2(0)^{b}	2(0)^{bc}	21(0)^{ab}	12(1)^{bd}	10(0)^{b}	14(1)^{a}	12(2)^{a}	2(0)^{ab}	2(1)^{a}	tr	1(0)
BC	22(1)^{b}	2(0)^{b}	3(1)^{ab}	22(1)^{ab}	12(0)^{bd}	9(0)^{c}	13(1)^{ab}	11(3)^{a}	1(0)^{bc}	3(1)^{a}	tr	2(0)
C	23(1)^{ab}	2(0)^{b}	2(0)^{bc}	22(2)^{a}	12(1)^{bd}	9(0)^{c}	14(0)^{a}	12(2)^{a}	tr	2(1)^{a}	tr	2(1)
T4, soil with thick cover made of Gramineae spp.												
A1	24(2)^{ab}	tr	–	20(1)^{ac}	10(1)^{de}	9(1)^{c}	13(1)^{ab}	15(2)^{a}	3(1)^{a}	3(0)^{a}	2(1)^{a}	1(0)
A2	24(1)^{ab}	3(1)^{a}	1(0)^{ce}	20(1)^{ac}	10(1)^{de}	9(0)^{c}	13(1)^{ab}	14(3)^{a}	1(0)^{bc}	3(0)^{a}	1(0)^{b}	1(0)
Bw1	24(1)^{ab}	1(0)^{c}	tr	20(0)^{ac}	13(1)^{ac}	9(0)^{c}	13(1)^{ab}	14(2)^{a}	1(0)^{bc}	2(1)^{a}	1(0)^{b}	2(0)
Bw2	23(1)^{ab}	1(0)^{c}	1(0)^{ce}	21(1)^{ab}	12(0)^{bd}	10(0)^{b}	14(1)^{a}	13(1)^{a}	1(0)^{bc}	2(0)^{a}	tr	2(0)
Bw3	23(1)^{ab}	1(0)^{c}	1(0)^{ce}	20(1)^{ac}	11(0)^{ce}	10(0)^{b}	14(0)^{a}	15(2)^{a}	1(0)^{bc}	2(0)^{a}	tr	2(0)
BC1	22(1)^{b}	1(0)^{c}	tr	20(1)^{ac}	12(1)^{bd}	10(0)^{b}	14(0)^{a}	15(2)^{a}	2(0)^{ab}	2(1)^{a}	tr	2(0)
BC2	22(1)^{b}	1(0)^{c}	tr	22(1)^{a}	13(0)^{ac}	10(0)^{b}	14(0)^{a}	12(0)^{a}	2(0)^{ab}	2(0)^{a}	tr	2(0)
C	22(1)^{b}	2(0)^{b}	1(0)^{ce}	22(1)^{a}	12(1)^{bd}	10(0)^{b}	14(1)^{a}	12(1)^{a}	1(0)^{bc}	2(1)^{a}	tr	2(0)

In each column, mean values with different letters significantly differ for $P < 0.05$.
C = calcite, D = dolomite, G = gypsum, Q = quartz, P = plagioclases, M = micas, K = kaolinite, HIV/HIS = mixture of hydroxy-interlayered vermiculite (HIV) and hydroxy-interlayered smectite (HIS) at various degree of polymerization, M–S = interstratified mica–smectite (mostly 2:1), S = smectites, V = vermiculites, OM = other minerals (amphiboles, serpentine, talc).
tr = <1%.

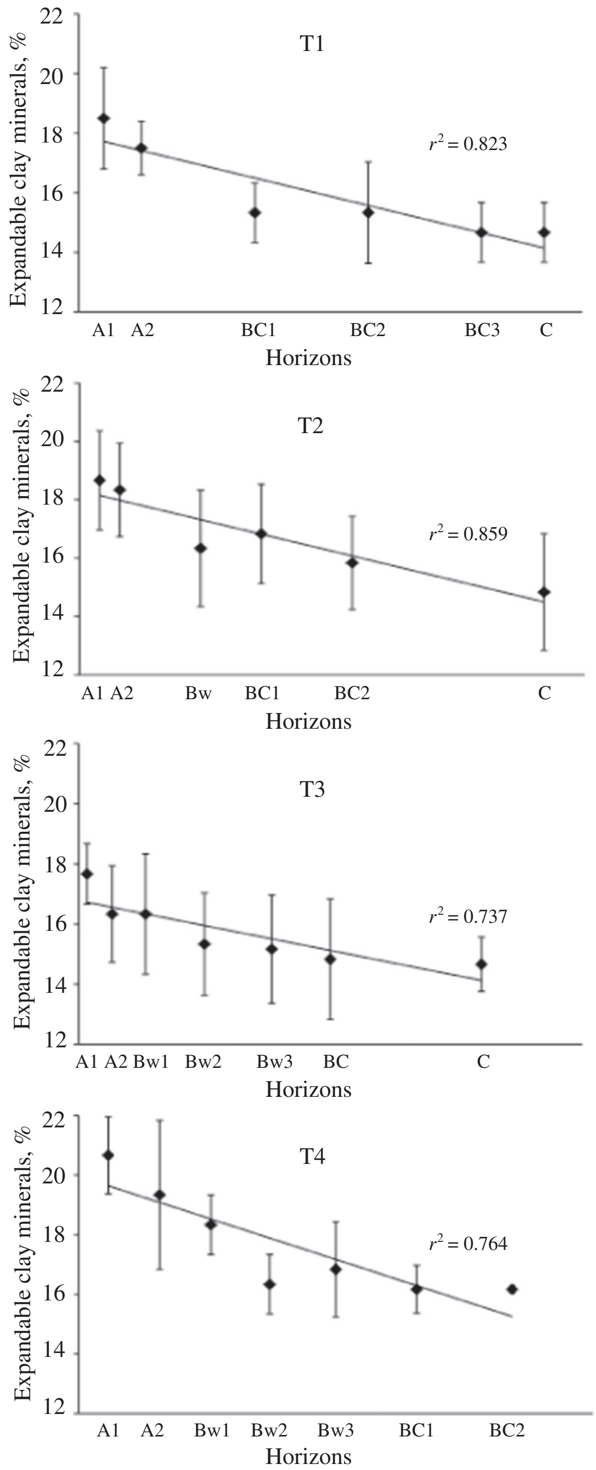

Fig. 6. Amounts of expandable clay minerals in the T1 to T4 soil profiles forming the land facets at Coste di Staffolo, Staffolo municipality (Ancona, Italy).

3.3. Mineralogy

In all the soils the predominant primary minerals were calcite, quartz, plagioclases (mainly of albitic composition), and micas (Table 3). As a whole, these minerals accounted for 61–67% of all the horizons. Other minerals such as dolomite and gypsum were present in small amounts. The most dominant clay minerals were kaolinite and HIV/HIS, followed by interstratified mica–smectite (mostly 2-to-1), smectites, and vermiculites. While some minerals (calcite, HIV/HIS, and smectites) were similarly diffused in all the profiles, others displayed their own highest content in different profiles (e.g., plagioclases in the Bw horizon of T2 soil; gypsum in the BC3 horizons of T1 soil and BC2 horizon of T2 soil). However, in no profile a clear trend with depth was observed for any mineral. The sum of the phyllosilicates (micas, kaolinite, HIV/HIS, interstratified mica–smectite, smectites, vermiculites, serpentine, and talc) gave values ranging from 39% and 46% for all soils, with no significant difference within and among the soils. The sum of expandable minerals, which were represented by smectites, vermiculites, HIV/HIS, and interstratified mica–smectite (its content was divided by 3 because of the 2-to-1 interlayering) showed a decreasing trend with depth, with r^2 always higher than 0.737 (Fig. 6).

3.4. Chemical properties

In all soils, the pH tended to increase with depth from sub-alkaline to alkaline values (Table 4). The lowest pH value (7.93) was measured in the A1 horizon of T4 soil, but in most other cases pH was higher than 8.5, which is the pH-threshold used to distinguish sodic soils from other salt-affected soils (Richards, 1954). The total C content showed no trend with depth in T1, T2, and T3 soils, where it ranged between 31.8 and 35.8 g kg^{-1} (Table 4), while in T4 soil the A1 horizon had a content higher than that of all the horizons below. Conversely to the general decreasing trend observed in T2, T3, and T4 soils, the organic C content of T1 soil increased from the A1 to the BC1 horizon and remained constant underneath (Table 4). Contrasting the whole soils, T1 and T2 contained less organic C than T3 and T4. The total N content showed no trend with depth in T1 and T2 soils, while in T3 and T4 soils it decreased with depth (Table 4). Further, total N concentration increased from T1 and T2 to T3 and T4 soils.

Table 4
pH in water, and content of total C, organic C and total N for the land facet forming the badlands of Coste di Staffolo, Ancona, Italy. Numbers in parentheses are the standard errors.

	$pH_{(H_2O)}$	Total C	Organic C	Total N
		g kg^{-1}		
T1, soil with popcorn and barren surface				
A1	8.54(0.02)^{h}	33.4(0.7)^{be}	3.6(0.1)^{m}	0.27(0.06)^{gj}
A2	8.55(0.03)^{h}	32.4(0.3)^{be}	4.0(0.2)^{km}	0.26(0.02)^{hj}
BC1	8.87(0.02)^{cd}	33.0(0.7)^{be}	4.6(0.2)^{ik}	0.24(0.05)^{ij}
BC2	8.65(0.03)^{f}	32.6(0.0)^{be}	4.5(0.2)^{ik}	0.26(0.00)^{hj}
BC3	8.76(0.04)^{e}	32.1(0.1)^{ce}	4.5(0.2)^{ik}	0.27(0.01)^{gj}
C	9.03(0.02)^{b}	34.7(1.0)^{be}	4.6(0.3)^{ik}	0.21(0.01)^{j}
T2, soil under sparse Hordeum maritimum, Hedisarium coronarium and biological crust				
A1	8.56(0.03)^{h}	33.1(0.3)^{be}	4.3(0.2)^{il}	0.35(0.00)^{fg}
A2	8.76(0.03)^{e}	32.6(0.7)^{be}	3.7(0.2)^{lm}	0.34(0.01)^{fh}
Bw	8.64(0.03)^{fg}	31.8(0.3)^{de}	2.9(0.2)^{n}	0.27(0.03)^{gj}
BC1	8.42(0.02)^{i}	32.8(0.0)^{be}	4.1(0.1)^{jm}	0.29(0.01)^{fj}
BC2	8.40(0.02)^{i}	32.4(0.3)^{be}	4.3(0.1)^{il}	0.31(0.01)^{fi}
C	9.05(0.03)^{ab}	33.2(0.0)^{be}	5.7(0.1)^{h}	0.32(0.00)^{fi}
T3, soil under good cover made of Hedisarium coronarium and few Gramineae				
A1	8.57(0.03)^{gh}	37.3(0.6)^{b}	8.5(0.2)^{c}	0.88(0.05)^{b}
A2	8.81(0.03)^{de}	34.7(0.4)^{be}	8.0(0.1)^{cd}	0.57(0.04)^{e}
Bw1	8.92(0.03)^{c}	32.6(6.6)^{be}	6.9(0.2)^{ef}	0.68(0.03)^{cd}
Bw2	8.84(0.02)^{d}	33.9(0.1)^{be}	8.3(0.4)^{c}	0.56(0.04)^{e}
Bw3	8.56(0.04)^{h}	35.8(0.1)^{bd}	8.5(0.1)^{c}	0.58(0.04)^{e}
BC	8.41(0.02)^{i}	30.3(5.1)^{e}	7.4(0.1)^{de}	0.37(0.01)^{f}
C	9.11(0.01)^{a}	34.3(0.2)^{be}	5.8(0.4)^{gh}	0.29(0.00)^{fj}
T4, soil under thick cover made of Gramineae spp.				
A1	7.93(0.03)^{j}	49.3(0.9)^{a}	18.8(0.4)^{a}	1.90(0.05)^{a}
A2	8.45(0.03)^{i}	36.5(0.1)^{bd}	9.3(0.2)^{b}	0.74(0.03)^{c}
Bw1	8.66(0.03)^{f}	36.8(0.1)^{bc}	6.4(0.1)^{fg}	0.62(0.01)^{de}
Bw2	8.83(0.02)^{de}	36.6(0.5)^{bd}	6.3(0.1)^{fh}	0.59(0.01)^{e}
Bw3	9.03(0.02)^{b}	34.3(0.2)^{be}	4.7(0.3)^{ij}	0.35(0.05)^{fg}
BC1	9.06(0.01)^{ab}	34.0(0.0)^{be}	4.9(0.1)^{i}	0.35(0.03)^{f}
BC2	9.07(0.01)^{ab}	33.4(0.1)^{be}	3.8(0.2)^{lm}	0.33(0.00)^{fh}
C	9.10(0.01)^{a}	33.8(0.3)^{be}	5.8(0.3)^{gh}	0.28(0.01)^{fj}

In each column, mean values with different letters significantly differ for $P < 0.05$.

Extractable Ca, Mg, K, Na, and Cl were reported in Table 5. In T1, T2, and T3 soils the extractable Ca decreased from the surface until a certain depth, then a reverse depth-trend occurred. The depth at which the reverse depth-trend occurred increased according to the sequence T1 < T2 < T3. Conversely, in T4 the amount of extractable Ca tended to decrease with depth. Extractable Mg in T1 soil increased from A1 to A2 and diminished in the horizons below, while in T3 soil it displayed no variation from the A1 to Bw2 horizons, increased in the Bw3 and BC horizons, and decreased underneath. In T2 and T4 soils the extractable Mg increased with depth. Extractable K showed similar values in the upper part of the soil and increased at the bottom in T1, T2, and T3. In T4 soil, extractable K displayed the highest values in the A1 and BC2 horizons. Extractable Na increased with depth in T1, T2, and T3 soils, while in T4 soil it showed no significant change from the surface until the Bw3 horizon and increased more with depth. Extractable Ca generally increased from T1 to T4 in the three superficial horizons, while extractable Mg, K, and Na followed the opposite trend. The total extractable cations tended to increase with depth in T1, T2 and T3 soils, while in T4 soil they decreased from A1 to the horizons below, to increase at depth and reach a value similar to that atop the soil. Also, the total extractable cations showed a decreasing trend from T1 to T4 soils, especially in the deepest BC horizon. *ESP* tended to increase with depth in all the soils, and to decrease from T1 to T4 soils especially in the A and Bw horizons, while in the BC horizons differences were small. With the exception of the A1 horizon of T3 soil and the A, Bw1 and Bw2 horizons of T4 soil, *ESP* assumed a value higher than 15%, which is the threshold used to distinguish soils among the salt-affected ones (Richards, 1954). The amount of Cl was similar in the four soils, with the highest concentrations in the C horizons, where it reached values from 81.8 to 85.6 mmol kg^{-1}.

4. Discussion

4.1. Soil features and mineralogy

As observed in many slopes, landslides leave a bare surface made of poorly weathered parent material. This surface may remain barren for decades following intense erosion, especially on smectite-bearing mudrocks (Clotet et al., 1988). Because of this, the depressed position of T1 with respect to the other tesserae indicated that: i) T1 formed after the occurrence of a landslide, and ii) it experienced intense erosion. In spite of the erosion, a small thickness of the superficial parent material has been weathered and converted in a popcorn surface associated with a network of desiccation micro-cracks (Regüés et al., 2000). The presence of a popcorn surface in badlands has been widely documented for many different sites (e.g., Cantón et al., 2001; Kasanin-Grubin and Bryan, 2007; Yair et al., 2013). The processes related to the formation of the popcorn surface are: 1) an initial lowering of the bulk density (Regüés et al., 2000), and 2) repeated wetting/drying and freezing/thawing cycles that, if associated with the presence of expandable minerals, favor the re-arrangement of the mineral particles (Bryan et al., 1984; Bowyer-Bower and Bryan, 1986; Pardini et al., 1995; Kasanin-Grubin, 2012). In T1, pedogenesis has been poor and plants were absent, but a possible evolution of this tessera toward T3 and T4 is expected. Although the discharging of runoff through the network of micro-rills and rills removes seeds and seedlings so preventing plant colonization (Cerdá and García-Fayos, 2002; Aerts et al., 2006), the irregularities of the surface represent an opportunity for seed fixation, also for those that do not produce adhering mucilage (Harper and St. Clair, 1985; Mücher et al., 1988; Gutterman and Shem-Tov, 1997). Plant colonization generally occurs when the slope is lower than a

Table 5
Extractable Ca, Mg, K, Na and Cl, total cations extracted, and *ESP* for the land facet forming the badlands of Coste di Staffolo, Ancona, Italy. Numbers in parentheses are the standard errors.

	Ca	Mg	K	Na	Cl	Total cations	*ESP*
	mmol kg^{-1}					mmol kg^{-1}	%
T1, soil with popcorn and barren surface							
A1	70.5(1.1)^{fh}	43.6(1.8)^{cd}	23.4(0.0)^{c}	45.8(7.0)^{ij}	2.0(0.2)^{a}	183.3(14.0)^{fh}	25.0(3.7)^{b}
A2	64.1(3.8)^{hj}	49.8(0.1)^{ab}	25.2(0.1)^{c}	86.5(5.0)^{e}	4.4(0.3)^{bc}	225.6(12.7)^{de}	38.3(3.1)^{ab}
BC1	57.5(1.4)^{jk}	39.0(1.9)^{fi}	25.1(0.6)^{c}	72.0(5.8)^{fg}	6.9(0.3)^{df}	193.6(13.6)^{fg}	37.2(3.1)^{ab}
BC2	83.4(4.4)^{cd}	38.9(1.1)^{fi}	24.8(0.1)^{c}	91.1(4.2)^{de}	7.7(0.5)^{f}	238.2(13.9)^{cd}	38.2(3.1)^{ab}
BC3	96.3(3.7)^{b}	38.7(0.4)^{fi}	30.0(0.2)^{b}	124.8(4.7)^{c}	11.6(0.8)^{h}	289.8(10.6)^{b}	43.1(3.0)^{a}
C	94.0(2.9)^{b}	35.8(0.3)^{hj}	40.9(1.0)^{a}	136.2(5.8)^{b}	81.8(0.5)^{i}	306.9(14.1)^{ab}	44.4(3.3)^{a}
T2, soil under sparse Hordeum maritimum, Hedisarium coronarium and biological crust							
A1	75.5(1.6)^{df}	35.2(0.8)^{ij}	15.6(3.0)^{eg}	25.4(3.6)^{km}	1.2(0.2)^{a}	151.7(12.7)^{il}	16.7(2.5)^{c}
A2	77.1(0.5)^{df}	38.5(0.0)^{fi}	14.3(2.1)^{eh}	40.7(3.7)^{j}	2.2(0.2)^{ab}	170.6(8.9)^{gi}	23.9(2.1)^{bc}
Bw	67.1(1.8)^{gi}	41.9(0.1)^{dg}	22.8(3.2)^{c}	56.1(6.5)^{hi}	4.4(0.2)^{bc}	187.9(22.1)^{fg}	29.9(3.7)^{b}
BC1	63.2(1.8)^{hj}	41.9(0.4)^{dg}	18.2(2.1)^{de}	71.1(3.5)^{fg}	7.2(0.4)^{ef}	194.4(11.4)^{fg}	36.6(2.2)^{ab}
BC2	76.3(3.4)^{df}	42.9(1.4)^{cf}	24.4(1.5)^{c}	101.5(3.3)^{d}	11.9(0.0)^{h}	245.1(13.6)^{cd}	41.4(2.6)^{ab}
C	n.d.	n.d.	n.d.	143.3(1.1)^{ab}	82.6(0.6)^{i}	n.d.	n.d.
T3, soil under good cover made of Hedisarium coronarium and few Gramineae							
A1	88.7(2.5)^{bc}	38.1(1.6)^{gi}	15.7(0.4)^{eg}	22.5(1.6)^{lm}	1.3(0.2)^{a}	165.0(8.6)^{hj}	13.6(1.7)^{d}
A2	82.9(2.1)^{cd}	37.4(1.6)^{hj}	14.1(0.0)^{eh}	25.9(0.6)^{kl}	1.6(0.2)^{a}	160.3(6.1)^{hk}	16.2(1.4)^{c}
Bw1	80.7(1.6)^{ce}	36.8(1.7)^{hj}	13.3(0.8)^{fh}	37.8(3.1)^{jk}	3.4(0.2)^{ac}	168.6(10.2)^{gj}	22.4(2.0)^{bc}
Bw2	69.8(9.4)^{fi}	33.4(2.1)^{jk}	11.0(2.1)^{h}	38.8(3.7)^{j}	4.6(0.3)^{cd}	153.0(24.5)^{il}	25.4(5.3)^{b}
Bw3	61.9(0.4)^{ij}	40.1(2.4)^{eh}	21.6(1.8)^{cd}	82.5(1.8)^{ef}	10.8(0.3)^{gh}	206.1(9.1)^{ef}	40.0(1.8)^{ab}
BC	63.4(2.4)^{hj}	42.9(0.6)^{cf}	24.8(1.3)^{c}	121.1(3.9)^{c}	12.4(0.7)^{h}	252.2(11.6)^{c}	48.0(2.4)^{a}
C	115.8(2.3)^{a}	35.9(2.2)^{hj}	29.6(1.6)^{b}	149.8(0.1)^{a}	85.6(0.6)^{j}	331.1(8.8)^{a}	45.2(1.8)^{a}
T4, soil under thick cover made of Gramineae spp.							
A1	123.1(1.4)^{a}	22.4(0.4)^{l}	21.8(0.9)^{cd}	12.8(4.5)^{m}	1.2(0.2)^{a}	180.1(10.0)^{fh}	7.1(2.4)^{e}
A2	96.1(1.2)^{b}	24.8(0.8)^{l}	13.4(0.2)^{fh}	13.2(4.1)^{m}	1.3(0.2)^{a}	147.5(8.9)^{il}	8.9(2.2)^{e}
Bw1	83.8(0.2)^{cd}	30.4(0.1)^{k}	12.6(0.1)^{fh}	15.8(3.2)^{lm}	1.7(0.2)^{a}	142.6(5.1)^{jl}	11.1(1.6)^{de}
Bw2	73.1(1.7)^{eg}	36.6(0.0)^{hj}	12.5(0.5)^{fh}	15.8(5.3)^{lm}	2.1(0.2)^{ab}	138.0(10.6)^{kl}	11.4(2.8)^{de}
Bw3	52.4(1.0)^{kl}	44.8(0.7)^{cd}	12.2(1.0)^{gh}	24.3(4.7)^{lm}	5.4(0.2)^{ce}	133.7(9.8)^{l}	18.2(2.5)^{c}
BC1	44.8(2.4)^{l}	47.1(2.1)^{ac}	16.5(1.7)^{ef}	44.9(5.7)^{ij}	9.1(0.5)^{fg}	153.3(16.8)^{il}	29.3(3.4)^{b}
BC2	47.3(1.1)^{l}	50.4(0.7)^{a}	21.0(1.6)^{cd}	66.2(6.0)^{gh}	10.8(0.5)^{gh}	184.9(13.3)^{fh}	35.8(3.2)^{ab}
C	n.d.	n.d.	n.d.	147.6(2.3)^{a}	83.6(0.6)^{ij}	n.d.	n.d.

ESP = Exchangeable sodium percentage.
In each column, mean values with different letters significantly differ for $P < 0.05$.
n.d. = not determined.

certain threshold that, for semi-arid environments, varies from ~41° to 63° (Bochet et al., 2009). Even though in our study site precipitation was higher than in a semi-arid environment, in the absence of agricultural disturbances within or in the closest surroundings of the calanchi, at slopes of ~35° crust and crack network may favor plant colonization and, farther, soil evolution. However, in T1, a poorly pedogenized soil has evolved also in the absence of plants. In addition to the A1 horizon representing the crust, the soil was made by another ochric horizon (A2) and two BC horizons, everything resting on the not weathered mudrock (C horizon). Also, the increase of organic C with increasing depth is typical of young soils when they developed from organic matter bearing sediments. According to Agnelli et al. (2002, 2008), during the first stage of pedogenesis microorganisms use "geologic" organic matter and, consequently, the beginning of soil evolution produces a drop in organic matter. Thus, in a more advanced stage, the organic C content will increase because of the introduction of pedogenic organic matter. In the A horizons, the formation of an angular blocky structure was attributed to the wetting/drying cycles responsible for the formation of the popcorn surface, but also to cycles of solubilization/precipitation of carbonates and gypsum that, after re-precipitation, act as cements (e.g., Shainberg et al., 1989; Bronick and Lal, 2005). In the BC horizons, the platy structure was inherited from sedimentary parent material (as in the C horizon), while the secondary angular blocky structure had a pedogenic origin.

Since T2 formed as a crown around T1 and was restricted to the micro-escarpment between T1 and T3, it was interpreted as a transition tessera. T2 soil was probably able to conserve a sufficient moisture level that enabled cyanobacteria, algae, and lichens to colonize this area. This "critical" moisture content was probably maintained also because of the faint shadow produced by the plants that sparsely colonized T2, and those of the adjacent T3. As the microorganisms forming the biological crust were able to fix atmospheric N, they were responsible for the enrichment of soil N and, at least in the A1 horizon, organic C (De Falco, 1995; Harper and Belnap, 2001). The improvement of the chemical soil conditions probably favored the entrance of pioneer plants like *Hordeum maritimum*. This early plant colonization likely accelerated the pedogenesis by improving the drainage through 1) the development of soil structure throughout the profile and 2) the increased flow of soil solution, which uses roots as preferential discharging paths (Cocco et al., 2013). As a consequence, a thin Bw horizon formed and cations were leached.

In T3 and, to a greater extent, T4, the development of a thick cover of *Hedisarium* and gramineae was able to enrich the upper soil horizons of organic C and total N, while roots favored aggregation of soil particles, porosity, and water movements throughout the soil (e.g., Fageria and Stone, 2006; Cocco et al., 2013). The gradual soil and vegetal evolution along the tessera sequence appeared induced by a progressive root colonization throughout the soils, and by the consequent formation of Bw horizons. However, while in the T1, T2 and T3 soils roots were absent in the A horizons probably because of disturbances due to wetting/drying and swelling/shrinking cycles, in the T4 soil roots colonized the A horizons as the thick vegetation cover ensured a firmer soil condition. The increasing thickness of the Bw horizons caused the transition from Entisols (T1 and T2) to Inceptisols (T3 and T4).

In soils derived from marine sediments, a tight correlation between cutan development and clay content can be difficult to obtain as the texture of each horizon is mostly inherited from the parent layer, and the clay content may vary considerably from layer to layer (Robinson and Phillips, 2001; Corti et al., 2011). As the horizons with the most developed cutans corresponded to those with the highest clay (or, in some cases, silt) content (Table 2), we considered both these features as mainly inherited from the parent layers. However, we cannot exclude that water penetrated these horizons and was able to mobilize fines. In T1 and T2 soils the mobilization of fines would have been favored by the blocky soil structure and crack network (Retallack, 2005), while in T3 and T4 it would have been fostered also by the plant roots, which act as preferential pathway for discharging water (Cocco et al., 2013). The occurrence of shiny cutans on the upper part of the larger roots present in T3 and T4 soils would support this hypothesis.

The mineralogical assemblage of the horizons appeared unrelated to pedogenic processes, but inherited from the parent layers from which

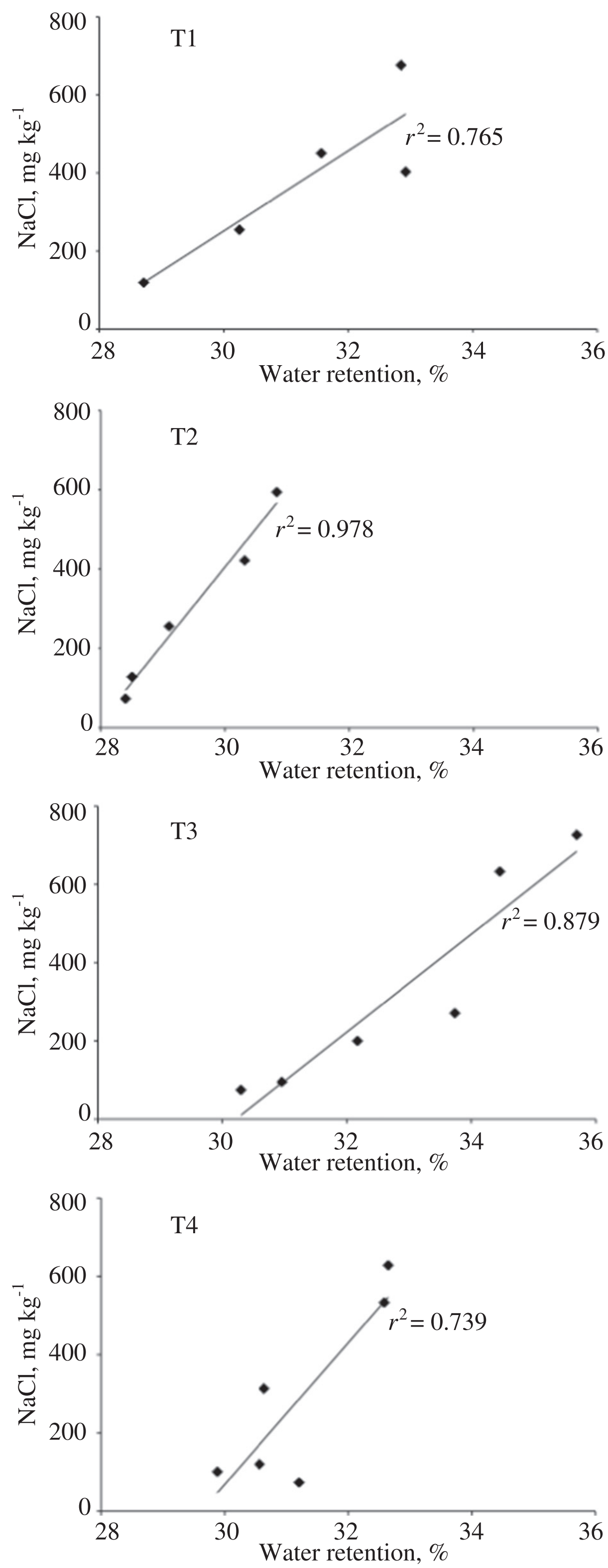

Fig. 7. Relationship between the content of NaCl and water retention at 33 kPa for the T1 to T4 soil profiles forming the land facets at Coste di Staffolo, Staffolo municipality (Ancona, Italy).

each horizon had formed (Battaglia et al., 2002; Kasanin-Grubin, 2012). The presence of the HIV/HIS mixture, which has been often found in marine sediments (e.g., Dypvik et al., 2003; Yin et al., 2013), supports the hypothesis that most of the minerals were inherited from the parent material. In fact, the pedogenic formation of HIV/HIS, especially in soils with low organic matter content, occurs because of intercalation of Al–OH polymers in the interlayers, and this is favored by the presence of Al ions in the soil solution (Karathanasis and Wells, 1989; Kämpf and Curi, 2003; Velde and Meunier, 2008). In contrast, the pH of our soils was so high to induce a low Al activity that allowed us to exclude that HIV/HIS can form in the actual soil environment. Further, from what has been possible to determine on a HIV/HIS mixture, in spite of pH changes along and among the profiles, the expandability level of these minerals did not vary substantially. Evidences like this have been reported by Azevedo et al. (1996), who did not observed any change in HIS expandability after 23 years of limestone applications (40 Mg ha^{-1} y^{-1}) to a tropical Oxisol. In contrast, changes of the HIV expandability level were observed in intensively grazed pastures where pH increase had been associated to urine concentration and manure distribution (Officer et al., 2006) or in a laboratory study when soil pH was raised from 3.6 and 5.4 to values higher than 7.2 (Niederbudde and Rühlicke, 1981). Evidently, the evolution of our soils has been so brief that, even in the most developed one (T4), mineral weathering produced no detectable modification. In effect, chemical conditions atop (A horizons) the T4 soil combined the highest amount of organic C with the lowest pH values, which are contrasting factors to obtain expandability level changes of HIV and HIS. Additional support to the hypothesis that soil mineral assemblage was mainly inherited from the parent material is the fact that no considerable difference occurred even for calcite, one of the most reactive minerals in soil.

Contrasting the morphology of the four soils, some clear tendencies appeared in the transition from T1 to T4: i) increases in the thickness of *solum* (A and B horizons) from 4–7 cm (T1) to ~35 cm (T4); ii) increased presence, even in the deeper horizons, and thickness of clay cutans; and iii) increased depth of the creeping cracks. Because of this, the four tesserae were considered as steps of an evolutionary trend that started after a landslide and brought forth the development of T4. This land facet formed because of a relatively long time of stable conditions, which was probably favored by moderate slope (~35°) and absence of agricultural disturbances.

4.2. Physical and chemical properties

Because of the pH values generally higher than 8.5 and *ESP* always larger than 15%, both T1 and T2 soils had a sodic character (Richards, 1954). This soil property may favor the clay dispersion, even though a considerable dispersion can be obtained when the ionic strength of the soil solution is below a certain level, which depends on the type of clay mineral and on the cationic composition of the solution (Kopittke et al., 2005). In T1 and T2 soils, the presence of cutans on the ped surface of few horizons indicated that, at these early stages of pedogenesis, a slight clay dispersion occurred. Judging from the relatively high concentration of extractable total cations, in T1 and T2 soils the ionic strength of the soil solution was sufficiently high to reduce the clay dispersion. Here, likely, a certain clay dispersion may occur only after prolonged rainfall events, when salt leaching has reduced the ionic strength of the soil solution. In T3 and, especially, T4 soils, the sodic character was less or was not expressed as *ESP* was lower than in T1 and T2 soils. Yet, in T3 and T4, the presence of cutans at the surface of peds and roots of many horizons was ascribed to a considerable clay dispersion due to the low ionic strength of the soil solution.

In these soils, water retention (Table 2) was not related with soil structure (Table 1) or clay content, which showed no significant difference with depth (Table 2). Water retention trend was not even related with phyllosilicate content, which did not vary throughout the profiles (Table 3), and did not depend on the amount of expandable minerals, which tend to decrease with depth (Fig. 6). This was different from the findings of many authors, who attributed the amount of water

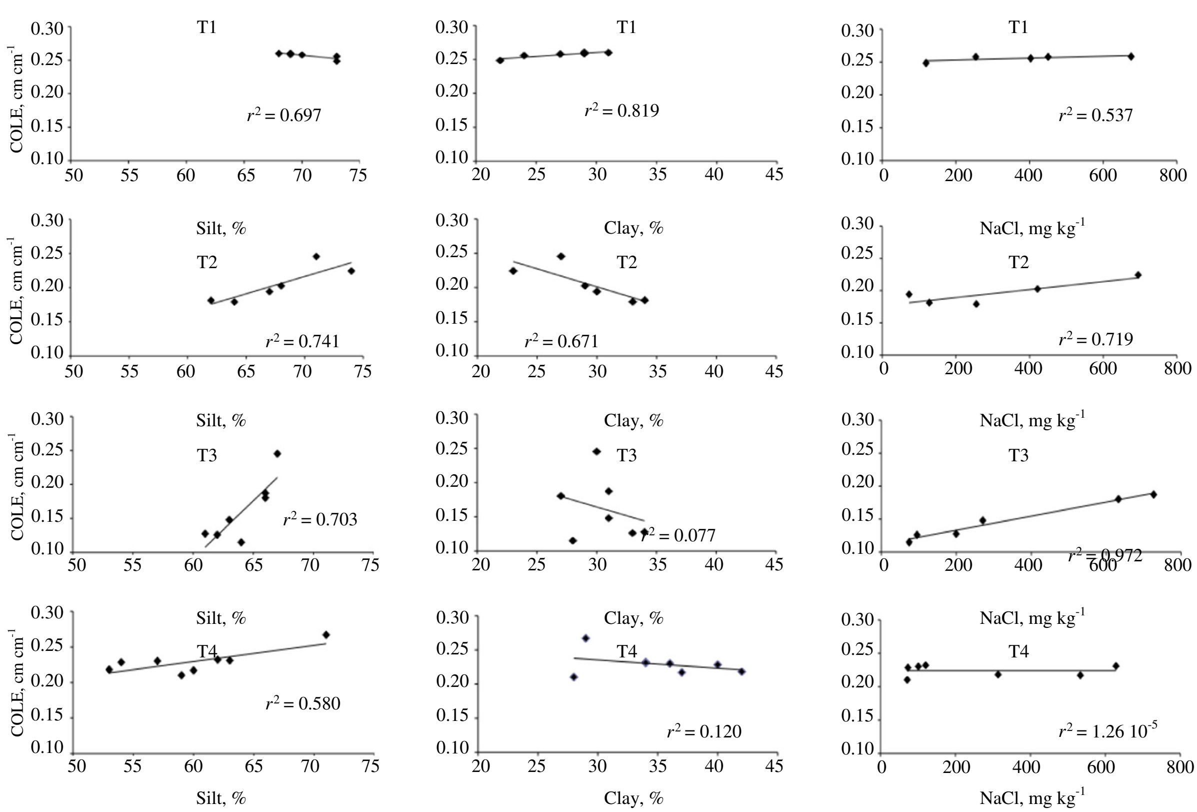

Fig. 8. Relationship between *COLE* and silt, clay or NaCl for the T1 to T4 soil profiles forming the land facets at Coste di Staffolo, Staffolo municipality (Ancona, Italy).

retention to the above mentioned ensemble of soil factors (e.g., Bruand and Tessier, 2000; Kodama, 2012; Mile and Mitkova, 2012; Wäldchen et al., 2012). Soil water retention at 33 kPa of our soils appeared related with the amount of NaCl salt (Fig. 7), as also reported, for example, by Abrol et al. (1988) and Ayers and Westcot (1994). On this aspect, additional considerations are needed. In these soils Na was always less than the sum of the other extractable cations. Further, Ca, Mg, and K have more affinity for exchangeable sites. Because of this, it is plausible that part of the extractable Na was not adsorbed on exchangeable sites, but was present as salt. At the sub-alkaline and alkaline pHs of these soils, it was expected that adsorption of anions was very scarce (e.g., Kafkafi et al., 2001) and, consequently, Cl was present as salt too. By assuming that all Cl was in form of NaCl, the estimated amount of this salt was 70–257 mg kg^{-1} in the A horizons, 99–631 mg kg^{-1} in the Bw horizons, 403–725 mg kg^{-1} in the BC horizons, and 4781–5003 mg kg^{-1} in the C horizons. The presence of NaCl in badlands has been widely reported (e.g., Ericksen et al., 1988; Piccarreta et al., 2006). Because of the sharp increment of NaCl salt from the BC to C horizons (which can be deduced by the Cl concentration shown in Table 5), the relation between water retention and NaCl content was significant when C horizons were omitted from plots (Fig. 7). In doing this, we obtained tendency lines with r^2 values of at least 0.739 (in the graph of T4 soil also the A1 horizon was eliminated). This would mean that, with a certain level of clay and clay minerals and little amounts of organic C, the NaCl content may affect water retention. Similar considerations were reported by Rajkai and Várallyay (1992) and Tóth et al. (2012). In the A horizons, the relatively small NaCl content was ascribed to the leaching, which was likely favored by progressive plant colonization from T1 to T4 soils and aggregate formation. Thus, in the first stage of pedogenesis (T1 and T2 soils) the formation of structure may be partly promoted, in addition to other factors, by salts through the increase of the ionic strength of the soil solution (Kopittke et al., 2005) and clay-ion bonding (Rengasamy and Olsson, 1991; Marchuk et al., 2013). In the more developed T3 and T4 soils the increase of organic matter is responsible for the structure of the upper horizons. The fact that plants start to colonize calanchi bare soils when the surface is relatively stabilized and the salt concentration is reduced has also been reported by Maccherini et al. (2011) and Torri et al. (2013). Continuing this process, the progressive increase of NaCl with depth in all soils was ascribed to the enhanced drainage and leaching favored by plants.

The *COLE* values were much higher than the limit of 0.09 cm cm^{-1} and consequently our soils were characterized by severe shrink–swell hazard (Lewis, 1979; Igwe and Okebalama, 2006). The *COLE* index depends on many soil variables. Parker et al. (1982) noted that the soil properties most related with *COLE* were the contents of swelling clays and clay, while the interstratified swelling clay, organic carbon, and sodium adsorption ratio were poorly related. Conversely, Reeve et al. (1980) found that *COLE* depended on organic C. In our soils, only inverse correlations were observed between *COLE* and content of expandable phyllosilicates, as these latter decreased and *COLE* increased with depth. In the T1 soil, reliable relations with *COLE* were observed only for clay, while in the other three soils *COLE* was well related with silt

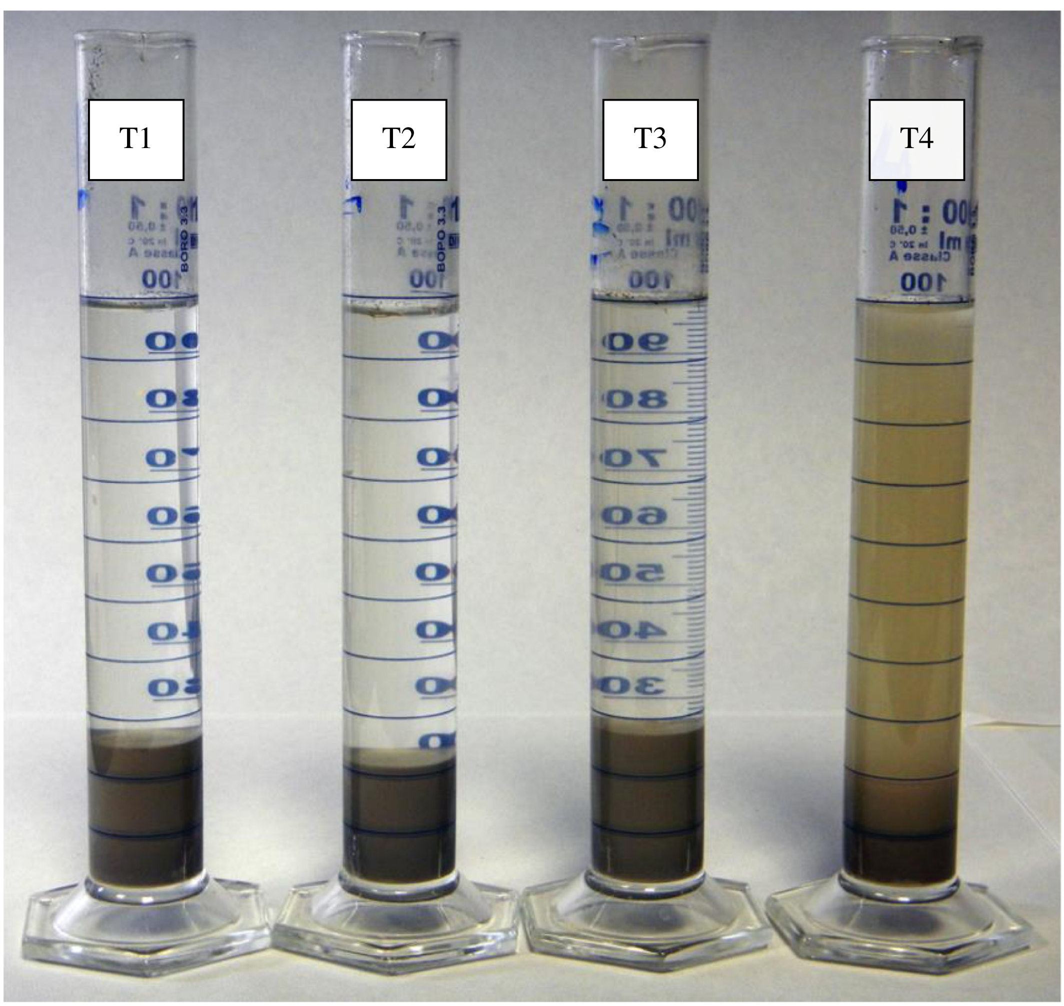

Fig. 9. Suspensions (15 g of soil to 100 mL of distilled water) obtained by using soil from BC2 horizon for T1, T2 and T4, and BC horizon for T3. Picture taken after 1 h from mixing indicates that clay of T1, T2 and T3 were flocculated, while that of T4 was dispersed.

and, with the exception of T4 soil, NaCl (Fig. 8). Importantly, the T1 soil had a relatively low clay content and a high Na content. A possible explanation of the relationships between *COLE* and clay in the T1 soil could be that clay was flocculated because of the high ionic strength of the soil solution (Kopittke et al., 2005; Chibowski, 2011). Likely, when clay is flocculated in presence of abundant Na, the larger the clay content, the greater the shrinking of the rod at the dry state. In the more developed T2, T3, and T4 soils, the decline of Na and the higher concentration of Ca probably had no relationship with clay, while the abundant silt, whose expansion is small and independent of salt concentration and type of saturating cation, induced a certain soil extensibility.

The soil behavior in terms of both water retention and *COLE* may explain the state of T1 soil. At the surface, water retention is limited so that water is rapidly lost, while extensibility and swelling are high. Such conditions exacerbate erosion and favor rapid drying of the extended and heaved soil surface, with the development of a popcorn and fractured surface. When pedogenesis has progressed, superficial erosion and formation of fractures and popcorn surface attenuate, while soil structure improves and organic matter content increases, so favoring water infiltration and salt leaching. Afterward, problems of soil stability progressively shift toward depth. Indeed, in the occasion of prolonged rainfall events, concentration of salts in the Bw and BC horizons declines because of leaching, and consequently, ionic strength of the soil solution drops below a certain threshold to induce clay dispersion. The possibility to achieve chemical conditions inducing clay dispersion in badlands as well as in other soil environments has been widely reported (e.g., Sherard and Decker, 1976; Goldberg et al., 1988; Faulkner, 2013). The higher clay dispersivity acquired by the BC horizon of the more developed T4 soil is shown in Fig. 9. Depending on the slope gradient, clay dispersion combined with the weight of the wet soil may trigger accelerated erosion.

5. Conclusions

Results of this study indicate that recognizing land facets in calanchi landscapes may help to understand the driving processes of soil genesis in these ecosystems, and to better define the role of soil evolution in the self-maintenance of calanchi. Field observations and laboratory data suggest that the pedogenesis in the calanchi may progress until a critical threshold. Advanced plant colonization and progressive root diffusion increase organic matter content and development of soil structure at depth, so favoring formation of *solum* and redistribution of nutrients along the profile. The improvement of structure at depth fosters water storage and, through soil leaching and reduction of the solution ionic strength, clay dispersion, to make the soil less stable. The progress of pedogenesis and development of vegetation cover make the soil even thicker and more porous, so that during the wet season it may contain enough water to become sufficiently heavy to overcome frictions that are reduced by clay dispersion at the level of the Bw or BC horizons. Depending on the slope gradient, the soil weight acquired during rainfall events may trigger landsliding, mudflows, or collapses. After these, the new barren surface will undergo pedogenic forces that will produce a new soil mantle. Therefore, along the calanchi slopes, tesserae with different degrees of soil and vegetal evolution are present, and pedogenesis alternates with sudden erosion phenomena that rejuvenate the surface. In areas where agricultural activity in the closest surroundings of the calanchi conveys rainfall water toward the flanks of the calanchi, tesserae with a rather developed soil may be induced to slide down as a consequence of the accelerated salt leaching (which favors clay dispersion) and soil overloading.

Acknowledgments

This work benefited of funds from the Cariverona Foundation (contract no. 2007.1508) and from the Marche Administrative Region (PSR Marche 2000–2006, Misura T). The authors are grateful to Luisa Massaccesi for her help in the statistical analysis of the data.

References

Abrol, I.P., Yadav, J.S.P., Massoud, F.I., 1988. Salt-affected soils and their managemen. FAO Soils Bulletin 39. Food and Agriculture Organization of the United Nations, Rome.

Aerts, R., Maes, W., November, E., Bahailu, M., Poesen, J., Deckers, J., Hermy, M., Muys, B., 2006. Surface runoff and seed trapping efficiency of shrubs in a regenerating semiarid woodland in northern Ethiopia. Catena 65, 61–70.

Agnelli, A., Celi, L., Degl'Innocenti, A., Corti, G., Ugolini, F.C., 2002. The changes with depth of humic and fulvic acids extracted from fine earth and rock fragments of a forest soil. Soil Sci. 167, 524–538.

Agnelli, A., Celi, L., Corti, G., Condello, L., 2008. Organic matter stabilization in soil aggregates and rock fragments as revealed by low-temperature ashing (LTA) oxidation. Soil Biol. Biochem. 40, 1379–1389.

Alexander, D.E., 1980. I calanchi — accelerated erosion in Italy. Geography 65, 95–100.

Alexander, D.E., 1982. Differences between "calanchi" and "biancane" badlands in Italy. In: Bryan, R., Yair, A. (Eds.), Badland Geomorphology and Piping. Geo Books, Norwich, pp. 71–87.

Alonso-Sarria, F., Romero-Díaz, A., Ruíz-Sinoga, J.D., Belmonte-Serrato, F., 2011. Gullies and badland landscapes in Neogene basins, region of Murcia, Spain. Landform Anal. 17, 161–165.

Ayers, R.S., Westcot, D.W., 1994. Water quality for agriculture. FAO Irrigation and Drainage Paper 29, Rev. 1. FAO, Rome.

Azevedo, A.C., Kämpf, N., Bohnen, H., 1996. Alterações na dinâmica evolutiva de Latossolo Bruno pela calagem. Rev. Bras. Ciênc. Solo 20, 191–198.

Battaglia, S., Leoni, L., Sartori, F., 2002. Mineralogical and grain size composition of clays developing calanchi and biancane erosional landforms. Geomorphology 49, 153–170.

Bochet, E., García-Fayos, P., Poesen, J., 2009. Topographic thresholds for plant colonization on semi-arid eroded soils. Earth Surf. Process. Landf. 34, 1758–1771.

Bowyer-Bower, T.A.S., Bryan, R.B., 1986. Rill initiation: concept and experimental evaluation on badland slopes. Z. Geomorphol. N.F. 60, 161–175.

Bridgewater, P.B., 1993. Landscape ecology, geographic information system and nature conservation. In: Haines-Young, R., Green, D.R., Cousins, S.H. (Eds.), Landscape Ecology and GIS. Taylor & Francis Ltd., New York, pp. 23–36.

Bronick, C.J., Lal, R., 2005. Soil structure and management: a review. Geoderma 124, 3–22.

Bruand, A., Tessier, D., 2000. Water retention properties of the clay in soils developed on clayey sediments: significance of parent material and soil history. Eur. J. Soil Sci. 51, 679–688.

Bryan, R.B., Yair, A., 1982. Perspectives on studies of badland geomorphology. In: Bryan, R., Yair, A. (Eds.), Badland Geomorphology and Piping. Geo Books, Norwich, pp. 1–12.

Bryan, R.B., Imeson, A.C., Campbell, I.A., 1984. Solute release and sediment entrainment on microcatchments in the Dinosaur park badlands, Alberta, Canada. J. Hydrol. 71, 79–106.

Bundy, L.G., Bremner, J.M., 1972. A simple titrimetric method for determination of inorganic carbon in soils. Soil Sci. Soc. Am. Proc. 36, 273–275.

Calzecchi-Onesti, A., 1954. Sistemazioni del Terreno e Fertilità in Collina. Ramo Editoriale Degli Agricoltori, Roma.

Cantón, Y., Domingo, F., Solé-Benet, A., Puigdefábregas, J., 2001. Hydrological and erosion response of a badland system in semiarid SE Spain. J. Hydrol. 252, 65–84.

Cantón, Y., Solé-Benet, A., Lázaro, R., 2003. Soil–geomorphology relations in gypsiferous materials of the Tabernas desert (Almería, SE Spain). Geoderma 115, 193–222.

Cerdá, A., García-Fayos, P., 2002. The influence of seed size and shape on their removal by water erosion. Catena 48, 293–301.

Chibowski, E., 2011. Flocculation and dispersion phenomena in soils. In: Gliński, J., Horabik, L., Lipiec, J. (Eds.), Encyclopedia of AgrophysicsEncyclopedia of Earth Sciences Series. Springer, Netherlands, pp. 301–304.

Clotet, N., Gallart, F., Balasch, J., 1988. Medium term erosion rates in a small scarcely vegetated catchment in the Pyrenees. Catena Suppl. 13, 37–47.

Cocco, S., Agnelli, A., Gobran, G.R., Corti, G., 2013. Changes induced by the roots of *Erica arborea* L. to create a suitable environment in a soil developed from alkaline and fine-textured marine sediments. Plant Soil 368, 297–313.

Corti, G., Agnelli, A., Ugolini, F.C., 1997. Release of Al by hydroxyl-interlayered vermiculite & hydroxy-interlayered smectite during determination of cation exchange capacity in fine earth and rock fragments fractions. Eur. J. Soil Sci. 48, 249–262.

Corti, G., Cavallo, E., Cocco, S., Biddoccu, M., Brecciaroli, G., Agnelli, A., 2011. Evaluation of erosion intensity and some of its consequences in vineyards from two hilly environments under a Mediterranean type of climate, Italy. In: Godone, D., Stanchi, S. (Eds.), Soil Erosion Issues in Agriculture. InTech, Rijeka, Croatia, pp. 113–160 (Chapter 6).

Corti, G., Cocco, S., Brecciaroli, G., Agnelli, A., Seddaiu, G., 2013. Italian soil management from antiquity to nowadays. In: Costantini, E.A.C., Dazzi, C. (Eds.), The Soils of ItalyWorld Soils Book Series. Springer, Netherlands, Dordrecht, pp. 247–293.

Cuniglio, R., Corti, G., Agnelli, A., 2009. Rock fragments evolution and nutrient release in vineyard soils developed on a thinly layered limestone (Tuscany, Italy). Geoderma 148, 375–383.

De Falco, L.A., 1995. Influence of Cryptobiotic Crusts on Winter Annuals and Foraging Movements of the Desert Tortoise (M.S. Thesis) Department of Biology, Colorado State University, Fort Collins, CO, USA.

de Santis, F., Giannossi, M.L., Summa, V., Tateo, F., 2010. Impact of physico-chemical soil properties on erosion features in the Aliano area (Southern Italy). Catena 81, 172–181.

Del Prete, M., Bentivenga, M., Amato, M., Basso, F., Tacconi, P., 1997. Badland erosion processes and their interactions with vegetation: a case study from Pisticci, Basilicata, Southern Italy. Geogr. Fis. Dinamica Quaternaria 20, 147–155.

Dramis, F., Gentili, B., Coltorti, M., Cherubini, C., 1982. Osservazioni geomorfologiche sui calanchi marchigiani. Geogr. Fis. Dinamica Quaternaria 5, 38–45.
Dypvik, H., Ferrell Jr., R.E., Sandbakken, P.T., 2003. The clay mineralogy of sediments related to the marine Mjølnir impact crater. Meteorit. Planet. Sci. 38, 1437–1450.
Ericksen, G.E., Hosterman, J.W., St. Amand, P., 1988. Chemistry, mineralogy and origin of the clay-hill nitrate deposits, Amargosa River Valley, Death Valley Region, California, U.S.A. Chem. Geol. 67, 85–102.
Fageria, N.K., Stone, L.F., 2006. Physical, chemical, and biological changes in the rhizosphere and nutrient availability. J. Plant Nutr. 29, 1327–1356.
Fairbridge, R.W. (Ed.), 1968. Encyclopedia of Geomorphology. Reinhold Book, New York.
Fascetti, S., Colacino, C., De Marco, G., 1990. Alcuni aspetti della vegetazione dei calanchi della Basilicata. 85° Congresso Società Botanica Italiana. G. Bot. Ital. 124, 144.
Faulkner, H., 2013. Badlands in marl lithologies: a field guide to soil dispersion, subsurface erosion and piping-origin gullies. Catena 106, 42–53.
Forman, R.T.T., Godron, M., 1986. Landscape Ecology. John Wiley & Sons, New York.
Gallart, F., Solé, A., Puigdefàbregas, J., Lázaro, R., 2002. Badland system in the Mediterranean. In: Bull, L.J., Kirkby, M.J. (Eds.), Dryland Rivers: Hydrology and Geomorphology of Semi-arid Channels. John Wiley & Sons, Ltd., Chichester, UK, pp. 299–326.
Gallart, F., Marignani, M., Pérez-Gallego, N., Santi, E., Maccheroni, S., 2013. Thirty years of studies on badlands, from physical to vegetational approaches. A succinct review. Catena 106, 4–11.
Godfrey, A.E., Everitt, B.L., Duque, J.F.M., 2008. Episodic sediment delivery and landscape connectivity in the Mancos Shale badlands and Fremont River system, Utah, USA. Geomorphology 102, 242–251.
Goldberg, S., Suarez, D.L., Glaubig, R.A., 1988. Factors affecting clay dispersion and aggregates stability of arid-zone soils. Soil Sci. 146, 317–325.
Guàrdia, R., Gallart, F., Ninot, J.M., 2000. Soil seed bank and seedling dynamics in badlands of the upper Llobregat basin (Pyrenees). Catena 40, 189–202.
Guasparri, G., 1993. Lineamenti Geomorfogici dei Terreni Argillosi Pliocenici. In: Giusti, F. (Ed.), La Storia Naturale della Toscana. Pizzi, Milano, pp. 89–106.
Gutterman, Y., Shem-Tov, S., 1997. Mucilaginous seed coat structure of *Carrichtera annua* and *Anastatica hierochuntica* from Negev Desert highlands of Israel, and its adhesion to the soil crust. J. Arid Environ. 35, 695–705.
Harper, K.T., Belnap, J., 2001. The influence of biological soil crusts on mineral uptake by associated seed plants. J. Arid Environ. 47, 347–357.
Harper, K.T., St. Clair, L.L., 1985. Cryptogamic soil crusts on arid and semiarid rangelands in Utah: effects on seedling establishment and soil stability. Final Report on BLM Contract No. BLMAA851-CT1-48. Department of Botany and Range Science, Brigham Young University, Provo, Utah. USA (archive.org/details/cryptogamicsoilc34harp).
Howard, A.D., 2009. Badlands and gullying. In: Parsons, A.J., Abrahams, A.D. (Eds.), Geomorphology of Desert Environments, Second edition Springer, Berlin, pp. 265–299.
Igwe, C.A., Okebalama, C.B., 2006. Soil strength of some Central Eastern Nigeria soils and effect of potassium and sodium on their dispersion. Int. Agrophys. 20, 107–112.
Imeson, A.C., Verstraten, J.M., 1988. Rills on badland slopes: a physico-chemically controlled phenomenon. Catena Suppl. 12, 139–150.
Kafkafi, U., Xu, G., Imas, P., Magen, H., Tarchitzky, J., 2001. Potassium and chloride in soils. In: Johnston, A.E. (Ed.), Potassium and Chloride in Crops and Soils: The Role of Potassium Chloride Fertilizer in Crop NutritionIPI Research Topics No. 22. International Potash Institute, Basel, Switzerland, pp. 29–48.
Kämpf, N., Curi, N., 2003. Argilominerais em solos brasileiros. In: Curi, N., Marques, J.J., Guilherme, L.R.G., Lima, J.M., Lopes, A.S., Alvares, V. (Eds.), Tópicos em ciência do solo. Sociedade Brasileira de Ciência do Solo, Viçosa, MG, pp. 1–54.
Karathanasis, A.D., Wells, K.L., 1989. A comparison of mineral weathering trends between two management systems on a catena of loess-derived soils. Soil Sci. Soc. Am. J. 53, 582–588.
Kasanin-Grubin, M., 2012. Clay mineralogy as a crucial factor in badland hillslope processes. Catena 106, 54–67.
Kasanin-Grubin, M., Bryan, R., 2007. Lithological properties and weathering response on badland hillslopes. Catena 70, 68–78.
King, R., 1990. Rural decline: the Mezzogiorno revisited. Geogr. Rev. 3, 7–10.
Kodama, H., 2012. Phyllosilicates. In: Huang, P.M., Li, Y., Sumner, M.E. (Eds.), Handbook of Soil Sciences — Properties and Processes, Second edition CRC Press, Taylor & Francis Group, Boca Raton, FL, pp. 21.1–21.49.
Kopittke, P.M., So, H.B., Menzies, N.W., 2005. Effect of ionic strength and clay mineralogy on Na–Ca exchange and the SAR–ESP relationship. Eur. J. Soil Sci. 57, 626–633.
Lavkulich, L.M., Wiens, J.H., 1970. Comparison of organic matter destruction by hydrogen peroxide and sodium hypochlorite and its effect on selected mineral constituents. Soil Sci. Soc. Am. Proc. 34, 755–758.
Lázaro, R., Alexander, R.W., Puigdefábregas, J., 2000. Cover distribution patterns of lichens, annuals and shrubs in the Tabernas Desert, Almería, Spain. In: Alexander, R.W., Millington, A.C. (Eds.), Vegetation Mapping: From Patch to Planet. Wiley, Chichester, pp. 19–39.
Lewis, D.J., 1979. Bulk density. In: Faibridge, R.W., Finkl Jr., C.W. (Eds.), Encyclopedia of Soil SciencePart I. Physics, Chemistry, Biology, Fertility and Technology. Dowden, Hutchinson and Ross, Stroudsburg, PA, pp. 47–48.
Maccherini, S., Marignani, M., Gioria, M., Renzi, M., Rocchini, D., Santi, E., Torri, D., Tundo, J., Honnay, O., 2011. Determinants of plants community composition of remnants biancane: a hierarchical approach to quantify species–environment relationships. Appl. Veg. Sci. 14, 378–387.
Marchuk, A., Rengasamy, P., McNeill, A., Kumar, A., 2013. Nature of the clay–cation bond affects soil structure as verified by X-ray computed tomography. Soil Res. 50, 638–644.
Martínez-Murillo, J.F., Nadal-Romero, E., Regüés, D., Cerdá, A., Poesen, J., 2012. Soil erosion and hydrology of the western Mediterranean badlands throughout rainfall simulation experiments: a review. Catena 106, 101–112.
McLeod, S., 1975. Studies on wet oxidation procedure for the determination of organic C in soil. Notes on Soil Techniques. CSIRO Division of Soil, Adelaide, Australia, pp. 73–79.
Mile, M., Mitkova, T., 2012. Soil moisture retention changes in terms of mineralogical composition of clay phase. In: Valaskova, M., Martynkova, G.S. (Eds.), Clay Minerals in Nature — Their Characterization, Modification and Application. InTech, Rijeka, Croatia, pp. 101–118 (Chapter 6).
Moretti, S., Rodolfi, G., 2000. A typical calanchi landscape of the Eastern Apennine margin (Atri, Central Italy): geomorphological features and evolution. Catena 40, 217–228.
Mücher, H.J., Chartres, C.J., Tongway, D.J., Greene, R.S.B., 1988. Micromorphology and significance of the surface crusts of soils in rangelands near Cobar, Australia. Geoderma 42, 227–244.
Niederbudde, E.A., Rühlicke, G., 1981. Umwandlung von Al-Chloriten durch Kalkung. Z. Pflanzenernähr. Bodenkd. 144, 127–135.
Officer, S.J., Tillman, R.W., Palmer, A.S., Whitton, J.S., 2006. Variability of clay mineralogy in two New Zealand steep-land topsoils under pasture. Geoderma 132, 427–440.
Pardini, G., Pini, R., Barbini, R., Regüés, D., Plana, F., Gallart, F., 1995. Laser elevation measurements of a smectite-rich mudrock following freeze–thawing and wet–drying cycles. Soil Technol. 8, 161–175.
Parker, J.C., Amos, D.F., Zelazny, L.W., 1982. Water adsorption and swelling of clay minerals in soil systems. Soil Sci. Soc. Am. J. 46, 450–456.
Pavari, A., 1911. Le crete senesi e lo scasso con la dinamite. L'Italia Agricola, Piacenza.
Phillips, C.P., 1998. The badlands of Italy: a vanishing landscape? Appl. Geogr. 18, 243–257.
Piccarreta, M., Faulkner, H., Bentivenga, M., Capolongo, D., 2006. The influence of physico-chemical material properties on erosion processes in the badlands of Basilicata, Southern Italy. Geomorphology 81, 235–251.
Plummer, C., Carlson, D., Hammersley, L., 2012. Physical Geology. Fourteenth edition. McGraw-Hill.
Rajkai, K., Várallyay, G., 1992. Estimating soil water retention from simpler properties by regression techniques. In: van Genuchten, M.T., Leij, F.J., Lunds, L.J. (Eds.), Methods for Estimating the Hydraulic Properties of Unsaturated soils. Proceedings of the International Workshop on Indirect Methods for Estimating the Hydraulic Properties of Unsaturated Soils, Riverside, California, 11–13 October 1989, pp. 417–426.
Reeve, M.J., Hall, G.G.M., Bullock, P., 1980. The effect of soil composition and environmental factors on the shrinkage of some clayey British soils. J. Soil Sci. 31, 429–442.
Regüés, D., Guàrdia, R., Gallart, F., 2000. Geomorphic agents versus vegetation spreading as causes of badland occurrence in a Mediterranean subhumid mountainous area. Catena 40, 173–187.
Rendell, H.M., 1986. Soil erosion and land degradation in southern Italy. In: Fantechi, R., Margaris, N.S. (Eds.), Desertification in Europe. Commission of European Communities, Brussels, pp. 184–193.
Rengasamy, P., Olsson, K.A., 1991. Sodicity and soil structure. Aust. J. Soil Sci. 29, 935–952.
Retallack, G.J., 2005. Soils — modern. In: Selley, R.C., Cocks, L.R.M., Plimer, I.R. (Eds.), Encyclopaedia of Geology. Elsevier Ltd., Amsterdam, pp. 194–202.
Richards, L.A. (Ed.), 1954. Saline and Alkali SoilsAgriculture Handbook No. 60. United States Salinity Laboratory Staff, United States Department of Agriculture. U.S. Government Printing Office, Washington, D.C.
Robinson, D.A., Phillips, C.P., 2001. Crust development in relation to vegetation and agricultural practice on erosion susceptible, dispersive clay soils from central and southern Italy. Soil Tillage Res. 60, 1–9.
Schafer, W.M., Singer, M.J., 1976. A new method of measuring shrink–swell potential using soil pastes. Soil Sci. Soc. Am. J. 40, 805–806.
Schoeneberger, P.J., Wysocki, D.A., Benham, E.C., Broderson, W.D. (Eds.), 2002. Field book for Describing and Sampling Soils. Version 2.0. Natural Resources Conservation Service, National Soil Survey Center, Lincoln, NE.
Shainberg, I., Sumner, M.E., Miller, W.P., Farina, M.P.W., Pavan, M.A., Fey, M.V., 1989. Use of gypsum on soils. A review. Adv. Soil Sci. 9, 1–111.
Sherard, J.L., Decker, R.S. (Eds.), 1976. Dispersive Clays, Related Piping, and Erosion in Geotechnical ProjectsASTM Special Technical Publication 623. American Society for Testing and Materials, Philadelphia, PA.
Soil Survey Staff, 2010. Keys to Soil Taxonomy. 11th edition. United States Department of Agriculture & Natural Resources Conservation Service, Washington, DC.
Summa, V., Tateo, F., Medici, L., Giannossi, M.L., 2007. The role of mineralogy, geochemistry and grain size in badland development in Pisticci (Basilicata, Southern Italy). Earth Surf. Process. Landf. 32, 980–997.
Torri, D., Regüés, D., Pellegrini, S., Bazzoffi, P., 1999. Within-storm soil surface dynamics and erosive effects of rainstorms. Catena 38, 131–150.
Torri, D., Santi, E., Marignani, M., Rossi, M., Borselli, L., Maccherini, S., 2013. The recurring cycles of biancana badlands: erosion, vegetation and human impact. Catena 106, 22–30.
Tóth, B., Makó, A., Guadagnini, A., Tóth, G., 2012. Water retention of salt-affected soils: quantitative estimation using soil survey information. Arid Land Res. Manag. 26, 103–121.
Velde, B., Meunier, A., 2008. The Origin of Clay Minerals in Soils and Weathered Rocks. Springer-Verlag.
Wäldchen, J., Schöning, I., Mund, M., Scrumpf, M., Bock, S., Herold, N., Totsche, K.U., Schulze, E.D., 2012. Estimation of clay content from easily measurable water content of air-dried soil. J. Plant Nutr. Soil Sci. 175, 367–376.
Yair, A., Bryan, R.B., Lavee, H., Schwanghart, W., Kuhn, N.J., 2013. The resilience of a badland area to climate change in an arid environment. Catena 106, 12–21.
Yin, K., Hong, H., Churchman, G.J., Li, R., Li, Z., Wang, C., Han, W., 2013. Hydroxy-interlayered vermiculite genesis in Jiujiang late–Pleistocene red earth sediments and significance to climate. Appl. Clay Sci. 74, 20–27.